DALTON

Synthesis, structure and reactivity of η^4(5e)-butadienyl substituted molybdenum complexes *

Arno Fries,[a] Michael Green,[a,b] Mary F. Mahon,[a] Thomas D. McGrath,[a] Caroline B. M. Nation,[a,b] Alan P. Walker[a] and Christopher M. Woolhouse[b]

[a] *School of Chemistry, University of Bath, Claverton Down, Bath BA2 7AY, UK*
[b] *Department of Chemistry, King's College London, Strand, London WC2R 2LS, UK*

Reaction of lithium halides with the cationic complexes [Mo(NCMe)(η^2-alkyne)$_2$L] (L = η-C_5H_5 or η^5-C_9H_7) afforded the halogeno-bis(alkyne) substituted molybdenum complexes [MoX(η^2-alkyne)$_2$L] (X = Cl, Br or I). A single-crystal X-ray diffraction study of the complex [MoI(η^2-MeC_2Me)$_2$(η-C_5H_5)] showed that the two alkyne ligands lie approximately parallel to the Mo–I vector and the plane of the η-C_5H_5 ligand. Reaction of [MoX(η^2-RC_2R)$_2$(η-C_5H_5)] with HBF_4·Et_2O afforded excellent yields of the aqua complexes [Mo{=C(R)-η^3-[C(R)C(R)CHR]}X(OH_2)(η-C_5H_5)][BF_4] (X = Cl, R = Me **9**; X = Cl, R = Et **10**; X = Br, R = Et **11** and X = I, R = Et **12**); a single-crystal X-ray diffraction study of the cation **11** confirmed the presence of co-ordinated H_2O and of a η^4(5e)-butadienyl fragment in an *anti*-supine conformation, the water occupying a co-ordination position *trans* to the Mo=C bond. The H_2O ligand in these cations can be displaced by acetonitrile allowing the synthesis of the complexes [Mo{=C(R)-η^3-[C(R)C(R)CHR]}X(NCMe)(η-C_5H_5)][BF_4] (X = Br, R = Me **13**; X = Br, R = Et **14** and X = I, R = Et **15**). A single-crystal structure determination of **14** confirmed the overall geometry of the complex and showed that the co-ordinated MeCN also occupies a position *trans* to the Mo=C bond. Treatment of the aqua complexes with LiX resulted in the formation of the neutral dihalogeno complexes [Mo{=C(R)-η^3-[C(R)C(R)CHR]}X_2(η-C_5H_5)] (X = Cl, R = Me **16**; X = Cl, R = Et **17**; X = Br, R = Et **18**; X = I, R = Et **19** and X = Br, R = Me **20**). The structure of **18** was confirmed by X-ray crystallography, and it was also found that the mixed dihalogeno complex [Mo{=C(Et)-η^3-[C(Et)C(Et)CHEt]}ClI(η-C_5H_5)] **21**, is formed in high yield on reaction of the acetonitrile-substituted complex **15** with LiCl. Reaction of trimethyl phosphite with the aqua- or acetonitrile-substituted cations resulted in the stereoselective formation of the complexes [Mo{=C(R)-η^3-[C(R)C(R)CHR]}X{$P(OMe)_3$}(η-C_5H_5)][BF_4] (X = Br, R = Me **23**; X = Cl, R = Me **24** and X = Br, R = Et **25**). A single-crystal X-ray study of **23** confirmed the presence of a cisoid *anti*-supine η^4(5e)-butadienyl ligand and also showed that the $P(OMe)_3$ ligand occupies a position *cis* to the Mo=C bond. In contrast, treatment of the aqua complexes with the poorer π-acceptor PMe_3 afforded isomeric mixtures of substitution products. However, reaction of complex **14** with PMe_3 afforded a complex which was structurally identified by X-ray crystallography as [Mo{=C(Et)-η^3-[C(Et)C(Et)CHEt]}Br(PMe_3)(η-C_5H_5)][BF_4] **26a** where the phosphine ligand is *cis* to the Mo=C bond. The base, Li[$N(SiMe_3)_2$], reacted with **24** to give the X-ray crystallographically identified, air-sensitive, η^4-vinylallene complex [MoCl{η^4-CH(Me)=C(Me)C(Me)=C=CH_2}{$P(OMe)_3$}(η-C_5H_5)] **28**, which upon treatment with HBF_4·Et_2O reformed the η^4(5e)-butadienyl complex **24**. When **23** was reacted with $AlHBu^i_2$ the 1,3-diene complex [MoBr{η^4-CH(Me)=C(Me)C(Me)=CH(Me)}{$P(OMe)_3$}(η-C_5H_5)] **29** was formed. Reaction of this air-sensitive molecule with [Ph_3C][BF_4] regenerated **23**. The structures and mechanisms of formation of these various new types of complexes are discussed.

In 1984 we reported[2] that reaction of the η^4-tetraphenylcyclobutadiene complex [Ru(NCMe)(η^4-C_4Ph_4)(η-C_5H_5)][BF_4] with K[$BHBu^s_3$] led to a ring-opening reaction and the formation of a purple crystalline air-sensitive complex. This was structurally identified by single-crystal X-ray crystallography as the first example of a cisoid η^4(5e)-butadienyl complex, the molecule [Ru{=C(Ph)-η^3-[C(Ph)C(Ph)CHPh]}(η-C_5H_5)]. Further studies[3] with this complex showed that the butadienyl fragment can change its bonding mode from η^4(5e) to η^3(3e) on reaction with a donor ligand, which highlighted the important concept that η^4(5e)-butadienyl can function as a latent or stored co-ordinatively unsaturated η^3(3e)-butadienyl, with consequences for reactivity studies. Subsequent to our initial report on the ruthenium system, it was shown that treatment of [W(η^2-PhC_2Ph)$_2$(η^2-S_2CNEt_2)] with HBF_4 followed by aqueous NEt_3 gives [W{=C(Ph)-η^3-[C(Ph)C(Ph)CHPh]}O(η^2-S_2CNEt_2)],[4] and reaction of [W{=C(CF_3)C(CF_3)SPr^i}(η^2-$CF_3C_2CF_3$)(η-C_5H_5)] with but-2-yne affords [W{=C(CF_3)-η^3-[C(CF_3)C(Me)C(Me)SPr^i]}(η-C_5H_5)].[5] More recent synthetic studies have confirmed the versatility of the cisoid η^4(5e)-butadienyl ligand in a variety of environments, it being found[6] that protonation (HBF_4·Et_2O) of [MoBr(η^2-MeC_2Me)$_2$(η^5-C_9H_7)] followed by addition of PMe_3 gives [Mo{=C(Me)-η^3-[C(Me)C(Me)CHMe]}Br(PMe_3)(η^5-C_9H_7)][BF_4], treatment of [W(NCMe)(η^2-PhC_2Ph)$_2$(η^4-C_4Ph_4)] with KOH–water affords [W{=C(Ph)-η^3-[C(Ph)C(Ph)CHPh]}{η^2-MeC(O)NH}(η^4-C_4Ph_4)],[7] and interestingly reaction of the alkyne hydrotris(3,5-dimethylpyrazoyl)borate [HB(dmpz)$_3$] complex [$NbCl_2$(η^2-PhC_2Ph){HB(dmpz)$_3$}] with CH_2=$CHCH_2MgCl$ gives[8] the η^4(5e)-butadienyl complex [Nb{=C(Ph)-η^3-[C(Ph)CHCHMe]}Cl{HB(dmpz)$_3$}]. In initial studies of the reactivity of η^2(4e)-bonded alkyne complexes of rhenium[9] we have recently also shown that reaction of [$ReBr_2${η^2(4e)-PhC_2Ph}(η-C_5H_5)] with *o*-diphenylphosphinostyrene and $AgBF_4$–tetrahydrofuran (thf) results in the formation of [Re{=C(Ph)-η^3-[C(Ph)CHCHC_6H_4-PPh_2-*o*]}(η-C_5H_5)][BF_4].[10] More significantly, treatment of [ReBr(η^2-PhC_2Ph)$_2$(η-C_5H_5)][PF_6] with Li[$BHEt_3$] affords the complex [Re{=C(Ph)-η^3-[C(Ph)C(Ph)CHPh]}Br(η-C_5H_5)], an interesting molecule containing a transoid η^4(5e)-butadienyl with a novel 'bent' rhenium to carbon bond.[11] This paper reports a detailed study of the protonation reactions[6] of the

* Reactions of co-ordinated ligands. Part 64.[1]

halogeno complexes [MoX(η^2-alkyne)$_2$(η-C_5H_5)], and an examination of some aspects of the reaction chemistry of the resulting η^4(5e)-butadienyl substituted complexes.

Results and Discussion

The starting point of the present investigation was to examine the scope of our earlier finding[6] that [MoCl(η^2-MeC_2Me)$_2$(η-C_5H_5)] **1** can be synthesised selectively by reaction of [Mo(NCMe)(η^2-MeC_2Me)$_2$(η-C_5H_5)][BF_4] with LiCl in tetrahydrofuran, earlier investigations[12] having shown that the thermal reaction of [MoCl(CO)$_3$(η-C_5H_5)] with but-2-yne affords **1** or a tetramethyl-1,4-benzoquinone complex depending on the reaction conditions. It was found, as is detailed in the Experimental section, that a range of halogenobis(alkyne) substituted molybdenum complexes of the general formula [MoX(η^2-alkyne)$_2$L] **1**–**8** can indeed be readily formed in moderate yield, the resulting air-stable compounds all being characterised by elemental analysis and NMR spectroscopy. In order to confirm the structural identity of one of these complexes, and to provide a basis for reactivity studies, a single-crystal X-ray diffraction study with a suitable crystal of [MoI(η^2-MeC_2Me)$_2$(η-C_5H_5)] **3** was carried out. This established the solid-state structure illustrated in Fig. 1, selected bond lengths and angles being listed in Table 1. As expected the but-2-yne ligands exhibit typical[12,13] carbon–molybdenum and carbon–carbon bond lengths, and bendback angles, and lie approximately parallel to the Mo–I vector and the plane of the η^5-C_5H_5 ligand.

Addition of a molar equivalent of HBF_4·Et_2O to a cooled (−78 °C) solution of [MoCl(η^2-MeC_2Me)$_2$(η-C_5H_5)] **1** in dichloromethane resulted in a change from yellow to purple on warming to room temperature, and work-up by recrystallisation afforded a good yield (70%) of a red crystalline cationic complex **9**. A preliminary examination of the ^{1}H NMR spectrum revealed resonances corresponding to one η-C_5H_5 ligand and three methyl environments (1:2:1 relative intensities), and significantly, the ^{13}C-{^{1}H} spectrum showed a low-field singlet resonance at δ 306.6, characteristic of a molybdenum to carbon double bond. It was initially thought that **9** was a cationic η^2(3e)-vinyl complex[6,14,15] with the molecular formula [Mo{=C(Me)CHMe}Cl(η^2-MeC_2Me)(η-C_5H_5)][BF_4], however, attempts to obtain a suitable crystal for an X-ray crystallographic study and hence elucidate the structure were unsuccessful. It was, therefore, decided to extend the protonation studies to other halogenobis(alkyne) complexes in the hope of obtaining X-ray quality crystals. It was found that addition (−78 °C) of HBF_4·Et_2O to [MoCl(η^2-EtC_2Et)$_2$(η-C_5H_5)] **4**, [MoBr(η^2-EtC_2Et)$_2$(η-C_5H_5)] **5** and [MoI(η^2-EtC_2Et)$_2$(η-C_5H_5)] **6** afforded good yields of the corresponding cationic complexes **10**, **11** and **12** respectively. The ^{1}H NMR spectra of these cations confirmed the presence of one η-C_5H_5 environment, and as in the case of **9**, the ^{13}C-{^{1}H} spectra showed one resonance at low field in the range δ 304–298. It was thought that the Mo=C carbon atoms in these cations had their origin in the co-ordinated hex-3-yne contact carbons present in the starting materials [MoX(η^2-EtC_2Et)$_2$(η-C_5H_5)], but it was interesting that the remaining three contact carbons, *i.e.* *C*Et resonances, occurred in the range δ 147.8–71.0, which was not consistent[16] with the presence of a η^2(4e)-alkyne ligand, *i.e.* a cation with the molecular formula [Mo{=C(Et)CHEt}X{η^2(4e)-EtC_2Et}(η-

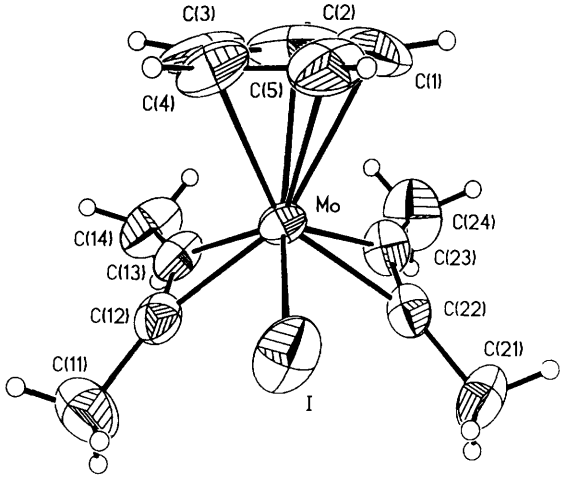

Fig. 1 Molecular structure of [MoI(η^2-MeC_2Me)$_2$(η-C_5H_5)] **3**. Ellipsoids are drawn at the 50% probability level

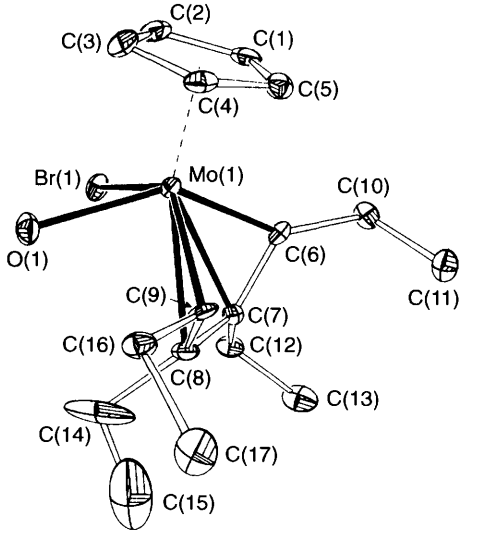

Fig. 2 Molecular structure of the cation present in [Mo{=C(Et)-η^3-[C(Et)C(Et)CHEt]}Br(OH_2)(η-C_5H_5)][BF_4] **11**. Ellipsoids are drawn at the 30% probability level

Table 1 Selected bond lengths (Å) and angles (°) for complex **3**

Mo–C(12)	2.061(6)	C(12)–C(13)	1.267(9)
Mo–C(13)	2.046(6)	C(22)–C(23)	1.279(8)
Mo–C(22)	2.065(6)	C(1)–C(2)	1.39(2)
Mo–C(23)	2.038(6)	C(2)–C(3)	1.367(14)
Mo–C(1)	2.399(8)	C(3)–C(4)	1.398(11)
Mo–C(2)	2.359(8)	C(11)–C(12)	1.496(9)
Mo–C(3)	2.379(7)	C(13)–C(14)	1.492(9)
Mo–C(4)	2.367(6)	C(21)–C(22)	1.482(8)
Mo–C(5)	2.373(7)	Mo–I	2.826(7)
C(11)–C(1)–C(13)	141.0(7)	C(21)–C(22)–C(23)	141.7(6)
C(12)–C(13)–C(14)	144.8(7)	C(22)–C(23)–C(24)	143.8(7)

Table 2 Selected bond lengths (Å) and angles (°) for complex **11**

Mo(1)–C(6)	1.993(9)	Mo(2)–C(6A)	1.913(13)
Mo(1)–O(1)	2.225(7)	Mo(2)–O(2)	2.245(8)
Mo(1)–C(9)	2.294(10)	Mo(2)–C(9A)	2.247(12)
Mo(1)–C(7)	2.341(10)	Mo(2)–C(7A)	2.303(11)
Mo(1)–C(8)	2.414(10)	Mo(2)–C(8A)	2.411(11)
Mo(1)–Br(1)	2.5786(1)	Mo(2)–Br(2)	2.579(2)
C(6)–C(7)	1.457(14)	C(6A)–C(7A)	1.41(2)
C(7)–C(8)	1.405(14)	C(7A)–C(8A)	1.41(2)
C(8)–C(9)	1.452(14)	C(8A)–C(9A)	1.42(2)
		C(9A)–C(16A)	1.52(2)
O(1)–Mo(1)–Br(1)	78.5(2)	O(2)–Mo(2)–Br(2)	75.8(2)
C(7)–C(6)–C(10)	126.5(9)	C(7A)–C(6A)–C(10A)	126.8(11)
C(8)–C(7)–C(6)	115.7(9)	C(8A)–C(7A)–C(6A)	115.8(10)
C(7)–C(8)–C(9)	116.3(9)	C(7A)–C(8A)–C(9A)	115.0(10)
C(8)–C(9)–C(16)	122.3(9)	C(8A)–C(9A)–C(16A)	123.8(12)

C_5H_5)][BF_4]. A possible explanation for the NMR data was that the co-ordinated hex-3-yne functioned as a two-electron donor and that the tetrafluoroborate anion was non-innocent,[17] *i.e.* a Mo(μ-F)B system was present, however, this was not supported by the variable-temperature ^{19}F NMR spectrum of **10**. This served to emphasise the importance of obtaining crystals of one of these cations suitable for an X-ray crystallographic study. Eventually suitable crystals of **11** were obtained by layer diffusion (CH_2Cl_2–pentane), the single-crystal structure determination establishing the molecular structure shown in Fig. 2, selected bond lengths and angles being listed in Table 2.

As suspected, the structure determination showed that complex **11** was not a η^2(3e)-vinyl–η^2(4e)-alkyne substituted complex, but that carbon–carbon bond formation had occurred, the

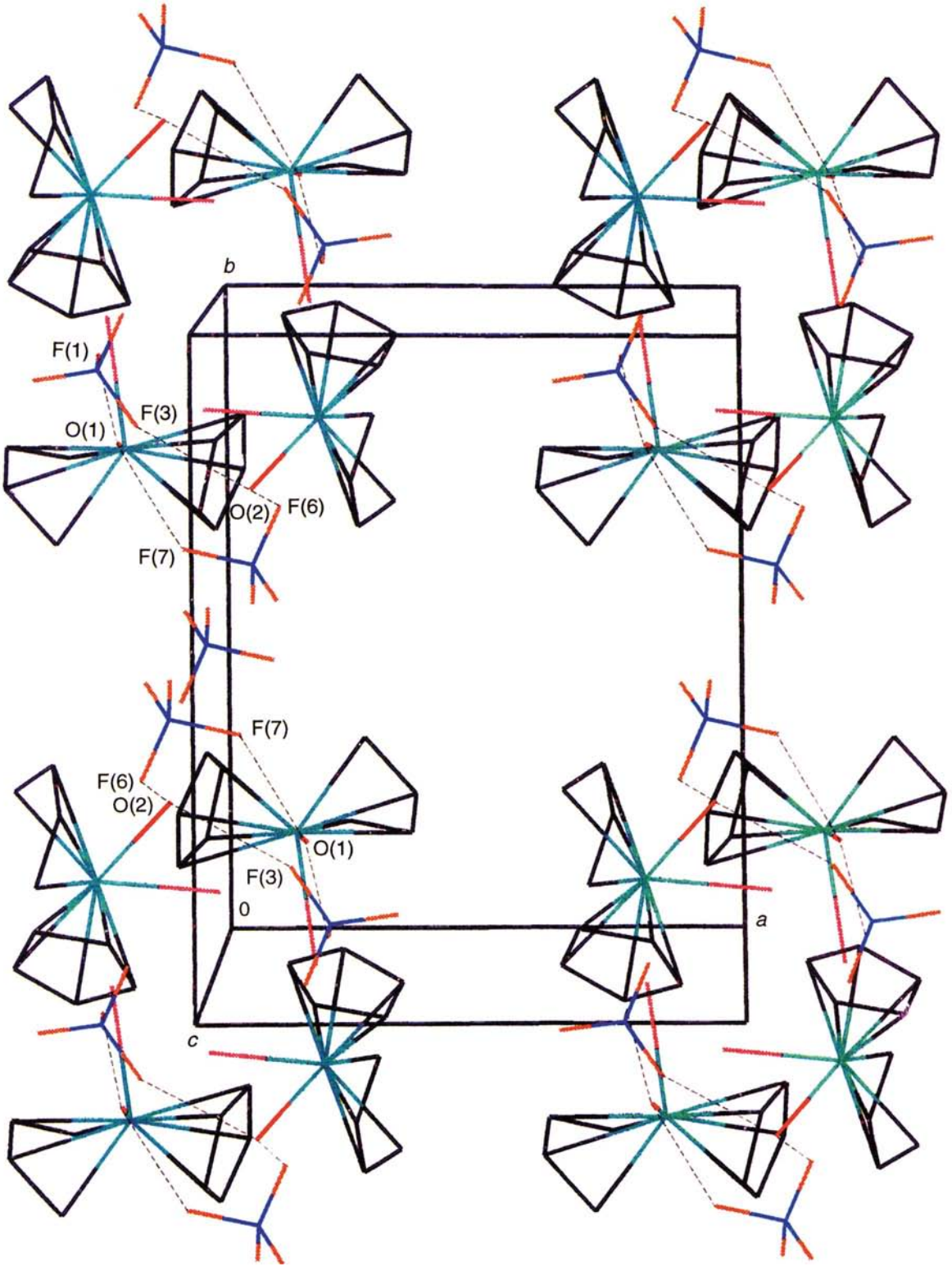

Green = Mo
Cyan = B
Orange = F
Red = O
Magenta = Br

Fig. 3 Packing diagram of complex **11**, ethyl groups omitted for clarity

molecule containing a cisoid η^4(5e)-butadienyl ligand in the *anti*-supine conformation along with a co-ordinated molecule of water. The Mo=C double bond [Mo–C(6) 1.933(9) Å], the C–C bonds of the butadienyl [C(6)–C(7) 1.47(1), C(7)–C(8) 1.41(1), C(8)–C(9) 1.45(1) Å] and the other bond parameters (see Tables 5 and 6) were similar to those found[3–6,10] in related complexes, the torsion angle C(6)–C(7)–C(8)–C(9) of −11.2° indicating a slight deviation from planarity for the C_4 backbone. As shown the H_2O ligand is *trans* to the Mo=C bond with C(6)–Mo(1)–O(1) 142.8(4)°, an interesting additional feature relating to the $MoOH_2$ system being the short F···O distances (in the range of 2.68–2.98 Å) indicating hydrogen bonding between the $[BF_4]$ anion and the co-ordinated water molecule. This feature is illustrated by the packing diagram shown in Fig. 3, and further discussed later in this manuscript.

With the structural identify of **11**, and by analogy that of **9**, **10** and **12**, established, it was then possible to re-examine the NMR data for these complexes and make detailed assignments (see Table 3). In the ^{1}H spectrum all four cations showed broad singlets in the range δ 3.95–4.16 and these resonances were assigned to the co-ordinated H_2O. Satisfactory elemental analyses were obtained in agreement with the illustrated structures (Scheme 1), the FAB mass spectra in the case of **9** and **11** showing peaks corresponding to the parent ion less H_2O.

In extending these protonation studies it was found that treatment of $[MoBr(\eta^2\text{-}MeC_2Me)_2(\eta\text{-}C_5H_5)]$ **2** with $HBF_4\cdot Et_2O$ gave a salmon red cationic complex. When however this was recrystallised from MeCN–Et_2O, a deep red crystalline complex **13** was obtained (80% yield). Elemental analysis and examination of the NMR spectra showed that **13** had the structure $[Mo\{=C(Me)\text{-}\eta^3\text{-}[C(Me)C(Me)CHMe]\}Br(NCMe)(\eta\text{-}C_5H_5)][BF_4]$. This implied that an initially formed aqua complex reacted with MeCN to give **13**. In agreement it was found that the aqua complexes **11** and **12** both reacted at room temperature with MeCN to give high yields of the acetonitrile-substituted complexes $[Mo\{=C(Et)\text{-}\eta^3\text{-}[C(Et)C(Et)CHEt]\}X(NCMe)(\eta\text{-}C_5H_5)][BF_3]$ **14** (X = Br) and **15** (X = I). Both cations were characterised by elemental analysis and NMR spectroscopy, and in order to define their stereochemistry a single-crystal X-ray diffraction study was carried out with a suitable crystal of **14**. The resulting structure is shown in Fig. 4, selected bond lengths and angles being listed in Table 4.

Thus, as is shown (Scheme 1), the replacement of the co-ordinated water molecule present in **11** by a nitrogen bonded acetonitrile takes place with retention of the *anti*-supine cisoid η^4(5e)-butadienyl geometry, the MeCN ligand occupying the same site, *i.e. trans* to the Mo=C bond, as was originally occupied by the displaced H_2O. Comparison of the molecular parameters of **11** and **14** (see Tables 5 and 6) showed that with the exception of a change in the planarity of the C_4 fragment

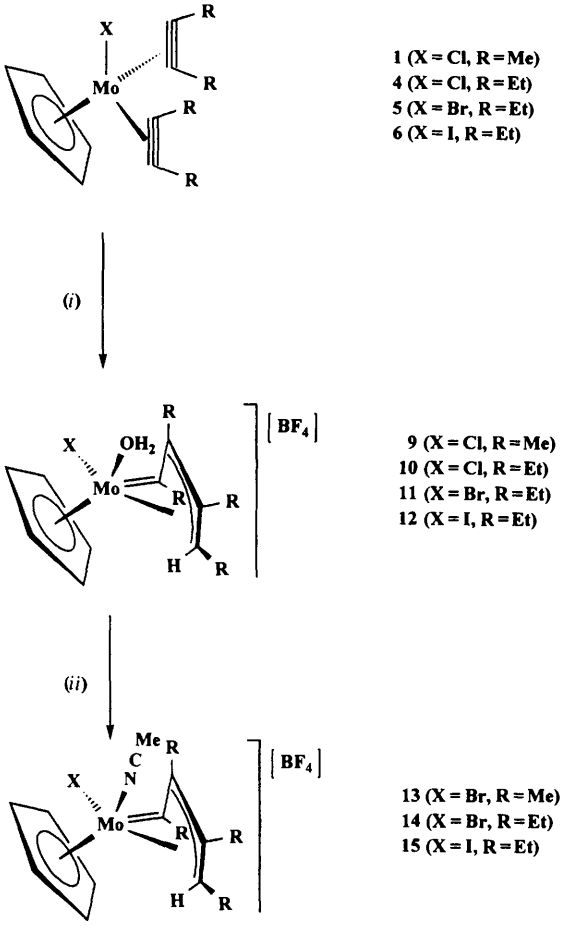

Scheme 1 (*i*) $HBF_4\cdot Et_2O$–water, CH_2Cl_2; (*ii*) +MeCN, $-H_2O$

Table 3 Carbon-13 NMR chemical shifts (ppm) for η^4(5e)-butadienylmolybdenum complexes

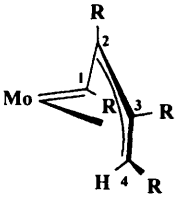

Complex	C^1	C^2	C^3	C^4
9 $[Mo\{=C(Me)\text{-}\eta^3\text{-}[C(Me)C(Me)CHMe]\}Cl(OH_2)(\eta\text{-}C_5H_5)][BF_4]$	306.6	135.6	115.1	73.8
10 $[Mo\{=C(Et)\text{-}\eta^3\text{-}[C(Et)C(Et)CHEt]\}Cl(OH_2)(\eta\text{-}C_5H_5)][BF_4]$	303.8	137.6	114.9	74.7
11 $[Mo\{=C(Et)\text{-}\eta^3\text{-}[C(Et)C(Et)CHEt]\}Br(OH_2)(\eta\text{-}C_5H_5)][BF_4]$	298.4	147.8	117.9	79.3
12 $[Mo\{=C(Et)\text{-}\eta^3\text{-}[C(Et)C(Et)CHEt]\}I(OH_2)(\eta\text{-}C_5H_5)][BF_4]$	302.2	132.5	108.0	71.0
13 $[Mo\{=C(Me)\text{-}\eta^3\text{-}[C(Me)C(Me)CHMe]\}Br(NCMe)(\eta\text{-}C_5H_5)][BF_4]$	297.3	140.7	120.1	74.4
14 $[Mo\{=C(Et)\text{-}\eta^3\text{-}[C(Et)C(Et)CHEt]\}Br(NCMe)(\eta\text{-}C_5H_5)][BF_4]$	297.4	140.2	119.3	79.5
15 $[Mo\{=C(Et)\text{-}\eta^3\text{-}[C(Et)C(Et)CHEt]\}I(NCMe)(\eta\text{-}C_5H_5)][BF_4]$	301.3	137.0	118.8	75.8
16 $[Mo\{=C(Me)\text{-}\eta^3\text{-}[C(Me)C(Me)CHMe]\}Cl_2(\eta\text{-}C_5H_5)]$	291.3	134.2	113.6	70.0
17 $[Mo\{=C(Et)\text{-}\eta^3\text{-}[C(Et)C(Et)CHEt]\}Cl_2(\eta\text{-}C_5H_5)]$	294.4	138.5	116.1	76.1
18 $[Mo\{=C(Et)\text{-}\eta^3\text{-}[C(Et)C(Et)CHEt]\}Br_2(\eta\text{-}C_5H_5)]$	295.3	136.7	113.8	74.5
19 $[Mo\{=C(Et)\text{-}\eta^3\text{-}[C(Et)C(Et)CHEt]\}I_2(\eta\text{-}C_5H_5)]$	295.5	134.2	110.0	70.6
20 $[Mo\{=C(Me)\text{-}\eta^3\text{-}[C(Me)C(Me)CHMe]\}Br_2(\eta\text{-}C_5H_5)]$	292.6	132.4	111.2	68.2
23 $[Mo\{=C(Me)\text{-}\eta^3\text{-}[C(Me)C(Me)CHMe]\}Br\{P(OMe)_3\}(\eta\text{-}C_5H_5)][BF_4]$	305.5	132.5	108.5	73.4
24 $[Mo\{=C(Me)\text{-}\eta^3\text{-}[C(Me)C(Me)CHMe]\}Cl\{P(OMe)_3\}(\eta\text{-}C_5H_5)][BF_4]$	305.2	132.7	108.7	75.1
26a $[Mo\{=C(Et)\text{-}\eta^3\text{-}[C(Et)C(Et)CHEt]\}Br(PMe)_3(\eta\text{-}C_5H_5)][BF_4]$	299.1	133.7	111.7	77.5

[torsion angle C(6)–C(7)–C(8)–C(9) 8.8(8)°], substitution of H_2O by MeCN results in relatively minor structural changes.

Subsequent to the establishment of the structural identity of the starting material **3** and of the aqua-substituted cation **11**, consideration could be given to establishing how the η^4(5e)-butadienyl ligand is formed on protonation of a bis(alkyne) complex; *i.e.* a $C_2 + C_2 \longrightarrow C_4$ reaction. It was reasonable to assume that the initial step in the reaction sequence involves delivery of a proton by $[Et_2OH][BF_4]$ to one of the contact carbons of a co-ordinated alkyne, this leading to the formation of, for example, the η^2(3e)-vinyl–η^2(4e)-alkyne substituted cation $[Mo\{=C(Et)CHEt\}Br\{\eta^2(4e)\text{-}EtCl_2Et\}(\eta\text{-}C_5H_5)][BF_4]$. There are then two possible reaction pathways available to this cation. In the first pathway it is suggested that this initial product reacts with a molecule of water, which is present either in the solvent or in the reagent $HBF_4{\cdot}Et_2O$, to form, *via* a switch in the bonding mode of the alkyne, the aqua complex $[Mo\{=C(Et)CHEt\}Br\{\eta^2(2e)\text{-}EtC_2Et\}(OH_2)(\eta\text{-}C_5H_5)][BF_4]$. Since the η^2(3e)-vinyl ligand which is present in this species contains a molybdenum to carbon double bond this aqua complex can be viewed as an η^2(2e)-alkyne–carbene complex related to the chromium complexes $[Cr\{=C(R)OMe\}\{\eta^2(2e)\text{-alkyne}\}(CO)_4]$ known to be involved in the Dötz cyclisation reaction.[18] In the early stages of the Dötz reaction a η^3-vinylcarbene is thought to be formed by coupling of the alkyne and carbene ligands, and it is interesting that calculations[19] have shown that the lowest energy pathway to the coupled η^3-vinylcarbene product is *via* an intermediate in which the co-ordinated alkyne is perpendicularly oriented relative to the chromium–carbene carbon vector. If a related perpendicular coupling reaction was to occur between the η^2(3e)-vinyl molybdenum to carbon double bond and the *cis*-co-ordinated alkyne present in the intermediate $[Mo\{=C(Et)CHEt\}Br\{\eta^2(2e)\text{-}EtC_2Et\}(OH_2)(\eta\text{-}C_5H_5)][BF_4]$, then as is shown in Scheme 2, the cisoid η^4(5e)-butadienyl ligand can be formed directly by coupling of the η^2-vinyl and alkyne ligands. However, as is also illustrated in Scheme 2, the direction of attack by the H_2O molecule, the orientation of the η^2(3e)-vinyl ligand and the stereochemistry of the initial protonation reaction control whether a *anti*-supine, *syn*-supine, *anti*-prone or *syn*-prone η^4(5e)-butadienyl complex is formed, and in order to gain an insight into why the *anti*-supine geometry is preferred, an extended-Hückel molecular orbital (EHMO) calculation was carried out on a $[MoX(\eta^2\text{-alkyne})_2(\eta\text{-}C_5H_5)]$ system using the molecular parameters established by X-ray crystallography for the complex $[MoI(\eta^2\text{-}MeC_2Me)_2(\eta\text{-}C_5H_5)]$ **3**.

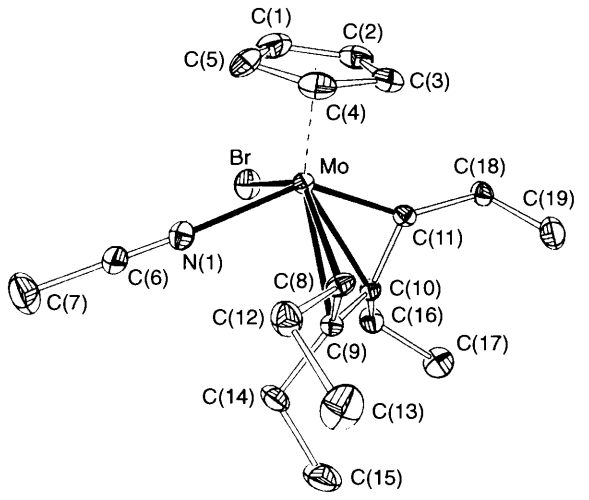

Fig. 4 Molecular structure of the cation present in $[Mo\{=C(Et)\text{-}\eta^3\text{-}[C(Et)C(Et)CHEt]\}Br(NCMe)(\eta\text{-}C_5H_5)][BF_4]$ **14**. Ellipsoids are drawn at the 30% probability level

Table 4 Selected bond lengths (Å) and angles (°) for complex **14**

Br–Mo	2.598(4)	C(8)–Mo	2.324(8)
N–Mo	2.201(8)	C(9)–Mo	2.431(8)
C(9)–C(8)	1.440(10)	C(10)–Mo	2.335(8)
C(10)–C(9)	1.390(9)	C(11)–Mo	1.925(8)
C(11)–C(10)	1.447(9)		
N–Mo–Br	79.2(2)	C(12)–C(8)–C(9)	123.6(6)
C(8)–Mo–N	78.4(3)	C(10)–C(9)–C(8)	117.8(6)
C(11)–Mo–Br	96.2(3)	C(11)–C(10)–C(9)	115.1(6)
C(18)–C(11)–Mo	147.4(5)		

Table 5 Bond lengths (Å) for η^4(5e)-butadienyl complexes

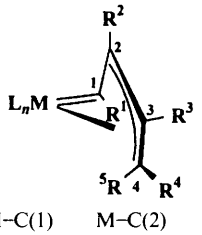

L_nM	R^1	R^2	R^3	R^4	R^5	M–C(1)	M–C(2)	M–C(3)	M–C(4)	C(1)–C(2)	C(2)–C(3)	C(3)–C(4)
$(\eta\text{-}C_5H_5)Ru$	Ph	Ph	Ph	H	Ph	1.896(5)	2.204(5)	2.152(4)	2.154(6)	1.419(5)	1.436(7)	1.445(7)
11 $(\eta\text{-}C_5H_5)(H_2O)BrMo$	Et	Et	Et	Et	H	1.933(9)	2.341(10)	2.414(10)	2.294(10)	1.467(14)	1.405(14)	1.452(14)
14 $(\eta\text{-}C_5H_5)(MeCN)BrMo$	Et	Et	Et	Et	H	1.925(8)	2.335(8)	2.431(8)	2.324(8)	1.447(9)	1.390(9)	1.440(10)
18 $(\eta\text{-}C_5H_5)Br_2Mo$	Et	Et	Et	Et	H	1.897(21)	2.310(24)	2.464(22)	2.281(25)	1.42(3)	1.45(3)	1.44(3)
23 $(\eta\text{-}C_5H_5)\{P(OMe)_3\}BrMo$	Me	Me	Me	Me	H	1.938(16)	2.352(19)	2.443(22)	2.336(23)	1.40(3)	1.40(3)	1.34(3)
26a $(\eta\text{-}C_5H_5)(PMe_3)BrMo$	Et	Et	Et	Et	H	1.930(9)	2.341(9)	2.467(9)	2.331(10)	1.434(11)	1.400(20)	1.429(12)

Table 6 Bond angles (°) for η^4(5e)-butadienyl complexes

L_nM	R^1	R^2	R^3	R^4	R^5	M–C(1)–C(2)	C(1)–C(2)–C(3)	C(2)–C(3)–C(4)	M–C(4)–C(3)	C(1)–C(2)–C(3)–C(4)
$(\eta\text{-}C_5H_5)Ru$	Ph	Ph	Ph	H	Ph	81.9(3)	119.4(3)	119.4(3)	70.3(3)	—
11 $(\eta\text{-}C_5H_5)(H_2O)BrMo$	Et	Et	Et	Et	H	86.1(6)	115.7(9)	116.3(9)	76.6(6)	−11.2
14 $(\eta\text{-}C_5H_5)(MeCN)BrMo$	Et	Et	Et	Et	H	86.5(5)	115.1(6)	117.8(6)	76.5(3)	8.8(8)
18 $(\eta\text{-}C_5H_5)Br_2Mo$	Et	Et	Et	Et	H	87(1)	115(2)	115(2)	80(2)	−4.9
23 $(\eta\text{-}C_5H_5)\{P(OMe)_3\}BrMo$	Me	Me	Me	Me	H	88(1)	114(2)	122(2)	78(1)	−4.4
26a $(\eta\text{-}C_5H_5)(PMe_3)BrMo$	Et	Et	Et	Et	H	86.9(5)	117.7(8)	118.1(8)	77.6(5)	−8.4(10)

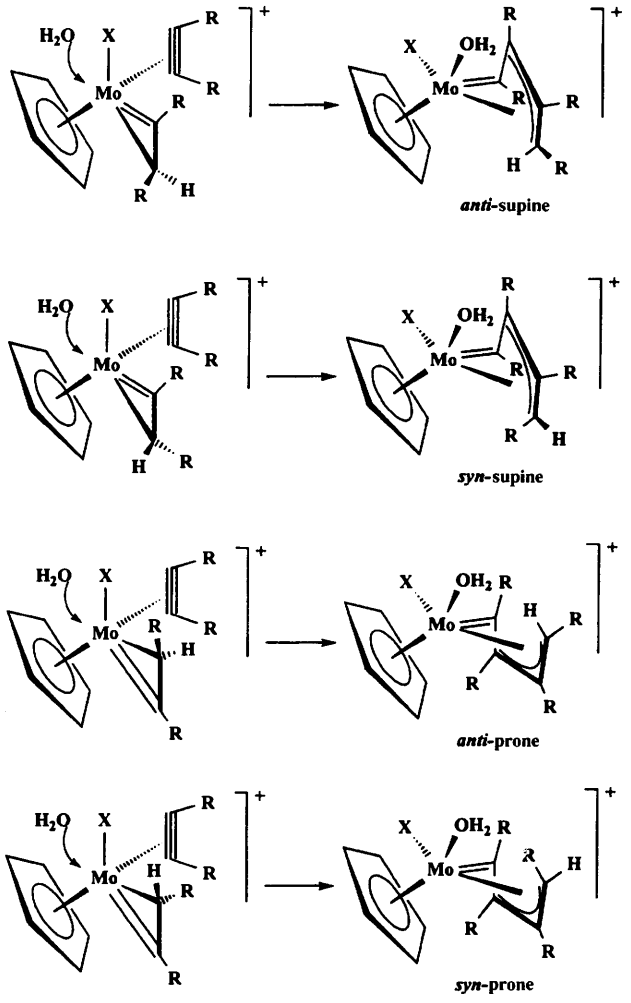

Scheme 2

Table 7 Charge densities (atomic units) on the alkyne contact carbons present in complex **3**

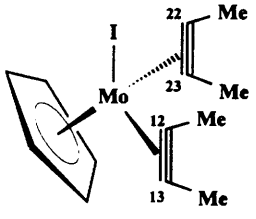

Atom	Net charge
C(12)	−0.4887
C(13)	−0.3459
C(22)	−0.4900
C(23)	−0.3482

The calculated charge densities on selected atoms are listed in Table 7, and with a view to assessing steric effects the space filling diagrams shown in Fig. 5 were generated for complex **3**. If the assumption is made that the protonation reaction is dominated by charge control then the relative charge densities suggest that attack should occur selectively at the alkyne contact carbons closest to the iodo ligand, *i.e.* C(12) and C(22), moreover, the space filling diagrams indicate that the preferred direction of attack is from the face opposite to the η-C_5H_5 ligand. However, as shown in Scheme 2, such a reaction path would lead to the *syn*-prone isomer, rather than the observed *anti*-supine. This implies that if this reaction pathway to the cisoid η^4(5e)-butadienyl ligand is actually followed, then the bulk of the reagent $[Et_2OH][BF_4]$ delivering the proton must override

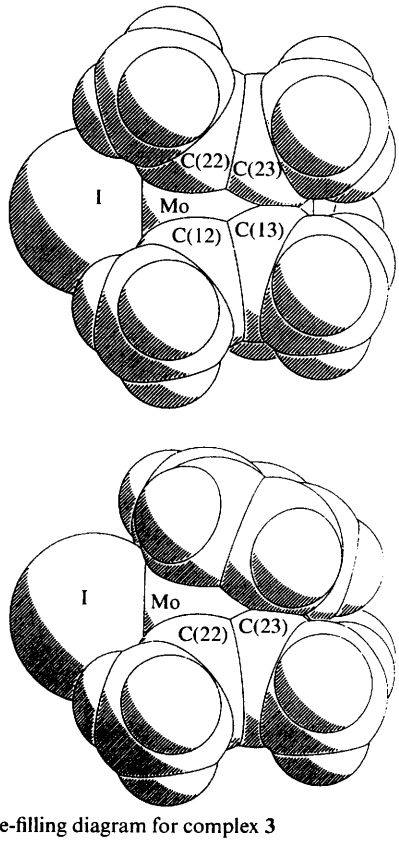

Fig. 5 Space-filling diagram for complex **3**

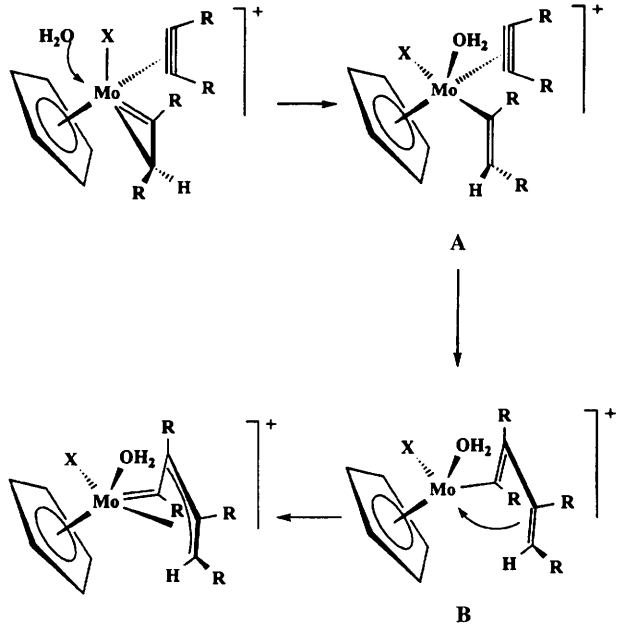

Scheme 3

simple charge density considerations with the result that either C(13) or C(23) are attacked from the side opposite to the cyclopentadienyl ligand leading to the formation of the isolated *anti*-supine product.

A second reaction pathway to the aqua η^4(5e)-butadienyl cations also requires the initially formed η^2(3e)-vinyl–η^2(4e)-alkyne substituted cationic complexes. This involves a rotational opening[14,20] of the η^2-vinyl to form a η^1-vinyl promoted by co-ordination of a water molecule. As is illustrated in Scheme 3, if the reasonable assumption is made that the σ-donor water molecule co-ordinates *trans* to the π-acceptor η^2(4e)-alkyne ligand, then the intermediate **A** can be formed. Migratory insertion of the η^1-vinyl onto the co-ordinated

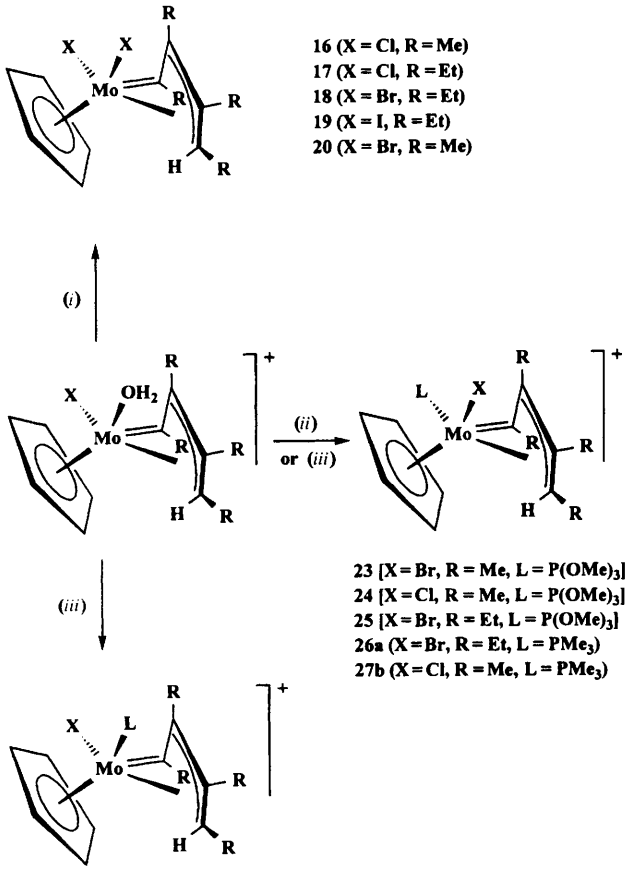

Scheme 4 BF_4^- counter anion. (*i*) LiX; (*ii*) $P(OMe)_3$; (*iii*) PMe_3

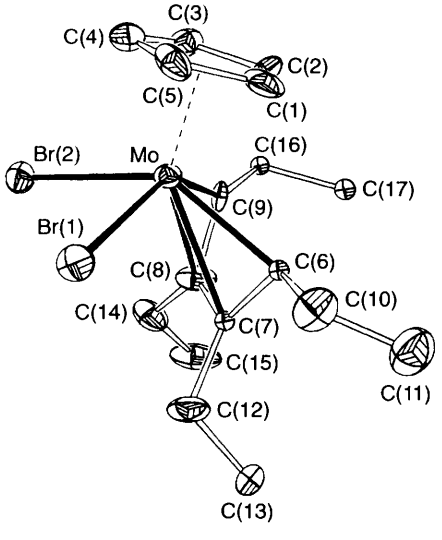

Fig. 6 Molecular structure of $[Mo\{=C(Et)-\eta^3-[C(Et)C(Et)CHEt]\}Br_2(\eta-C_5H_5)]$ **18**. Ellipsoids are drawn at the 30% probability level

alkyne then provides access to the 16e η^3(3e)-bonded butadienyl complex **B**, which can undergo an electronic reorganisation[3] to form the isolated aqua cisoid η^4(5e)-butadienyl substituted cation. It is not possible at present to differentiate between these two pathways, except it is interesting to note that there are no clearly defined examples of η^2(4e)-alkyne ligands undergoing migratory insertion reactions, which might indicate that the first pathway is followed.

The reactivity of the aqua complexes **9**–**12** towards acetonitrile suggested that it would be worthwhile to study their

Table 8 Selected bond lengths (Å) and angles (°) for complex **18**

Br(1)–Mo	2.648(6)	C(6)–Mo	2.28(3)
Br(2)–Mo	2.611(7)	C(7)–Mo	2.46(2)
C(7)–C(6)	1.43(3)	C(8)–Mo	2.32(2)
C(8)–C(7)	1.45(4)	C(9)–Mo	1.89(2)
C(9)–C(8)	1.43(3)		
Br(2)–Mo–Br(1)	80.5(2)	C(10)–C(6)–C(7)	119.8(22)
C(16)–C(9)–Mo	148.9(16)	C(8)–C(7)–C(6)	115.3(21)
C(16)–C(9)–C(8)	123.6(19)	C(9)–C(8)–C(7)	113.3(24)

reactivity towards other ligands (see Scheme 4). It was observed that the chloro-substituted cations **9** and **10** both reacted rapidly at room temperature with anhydrous lithium chloride in dichloromethane or CH_2Cl_2–thf as solvent to give good yields of the purple and red crystalline neutral complexes $[Mo\{=C(R)-\eta^3-[C(R)C(R)CHR]\}Cl_2(\eta-C_5H_5)]$ **16** (R = Me) and **17** (R = Et), molecules which can be viewed as analogues of the bis(cyclopentadienyl) complexes $[MoX_2(\eta^5-C_5H_5)_2]$. Similar reactions between the bromo- and iodo-substituted cations **11** and **12** with anhydrous LiBr or LiI respectively also afforded good yields of the corresponding neutral dibromo **18** and diiodo **19** complexes. Elemental analysis and NMR spectroscopy indicated that these reactions were selective and that the cisoid η^4(5e)-butadienyl ligand retained its structural integrity. In order to confirm this, a single-crystal X-ray diffraction study was carried out on complex **18**, the resulting structure is shown in Fig. 6, selected bond lengths and angles being listed in Table 8. The *anti*-supine geometry of the η^4(5e)-butadienyl ligand is retained and comparison of the bond parameters of **18** with those observed for **11** and **14** (see Tables 5 and 6) show that there are only minor changes. Thus, the neutral dibromo complex **18** has a shorter Mo=C bond, and there is a change in the planarity of the cisoid C_4 ligand as indicated by the torsion angle for C(1)–C(2)–C(3)–C(4) in **18** of −4.9°.

As expected the co-ordinated acetonitrile present in the cations $[Mo\{=C(R)-\eta^3-[C(R)C(R)CHR]\}X(NCMe)(\eta-C_5H_5)][BF_4]$ **13** (X = Br, R = Me), **14** (X = Br, R = Et) and **15** (X = I, R = Et) is also labile, this being demonstrated by the observation that within minutes the ^1H NMR spectra of solutions of the cations in CD_3CN showed only an unco-ordinated MeCN resonance. Addition of LiBr to $[Mo\{=C(Me)-\eta^3-[C(Me)C(Me)CHMe]\}Br(NCMe)(\eta-C_5H_5)][BF_4]$ **13** afforded the dibromo complex $[Mo\{=C(Me)-\eta^3-[C(Me)C(Me)CHMe]\}Br_2(\eta-C_5H_5)]$ **20**, and interestingly, the iodo-substituted cation **15** reacted regioselectively with LiCl to give a quantitative yield of the unsymmetrically substituted dihalogeno complex $[Mo\{=C(Et)-\eta^3-[C(Et)C(Et)CHEt]\}ClI(\eta-C_5H_5)]$ **21**. In contrast, when **14** was reacted with LiI a mixture of the diiodo complex **19** (major) and the bromo–iodo compound $[Mo\{=C(Et)-\eta^3-[C(Et)C(Et)CHEt]\}BrI(\eta-C_5H_5)]$ **22** (minor) were formed. It was also observed that longer reaction times led to the formation of only **19**. Unfortunately crystals suitable for X-ray crystallography of **21** could not be obtained, and therefore the stereochemistry of these displacement reactions could not be determined.

Fortunately, this was not a problem in the case of the reactions of the aqua- and acetonitrile-substituted cations with phosphorus-donor ligands (Scheme 4). Addition at room temperature of trimethyl phosphite to $[Mo\{=C(Me)-\eta^3-[C(Me)C(Me)CHMe]\}Br(NCMe)(\eta-C_5H_5)][BF_4]$ **13** resulted in a rapid change from deep red to bright orange, and the formation in high yield of the orange crystalline complex **23**. This analysed correctly for the complex $[Mo\{=C(Me)-\eta^3-[C(Me)C(Me)CHMe]\}Br\{P(OMe)_3\}(\eta-C_5H_5)][BF_4]$, and examination of the ^1H, $^{13}C-\{^1H\}$ and $^{31}P-\{^1H\}$ NMR spectra provided support for this structure. A reaction between the aqua complex $[Mo\{=C(Me)-\eta^3-[C(Me)C(Me)CHMe]\}Cl(OH_2)(\eta-C_5H_5)][BF_4]$ **9** and $P(OMe)_3$ proceeded in a similar stereospecific way

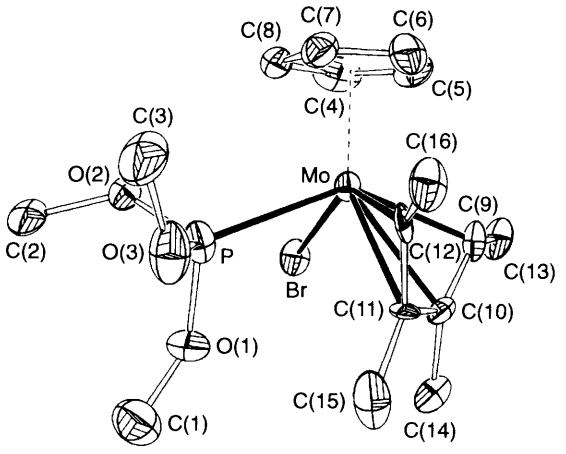

Fig. 7 Molecular structure of the cation present in $[Mo\{=C(Me)\text{-}\eta^3\text{-}[C(Me)C(Me)CHMe]\}Br\{P(OMe)_3\}(\eta\text{-}C_5H_5)][BF_4]$ **23**. Ellipsoids are drawn at the 30% probability level

Table 9 Selected bond lengths (Å) and angles (°) for complex **23**

Br–Mo	2.647(6)	C(10)–C(9)	1.37(3)
P–Mo	2.496(8)	C(13)–C(9)	1.52(3)
C(9)–Mo	2.32(2)	C(11)–C(10)	1.41(3)
C(10)–Mo	2.45(2)	C(12)–C(11)	1.42(3)
C(11)–Mo	2.36(2)	C(16)–C(12)	1.53(3)
C(12)–Mo	1.94(2)		
P–Mo–Br	79.5(3)	C(12)–C(11)–C(10)	113(2)
C(13)–C(9)–C(10)	123(2)	C(16)–C(12)–C(11)	131(2)
C(11)–C(10)–C(9)	121(2)		

to form the chloro analogue **24**. Analogous reactions between the aqua complex **11** or the acetonitrile-substituted complex **14** and trimethyl phosphite gave excellent yields of the cation $[Mo\{=C(Et)\text{-}\eta^3\text{-}[C(Et)C(Et)CHEt]\}Br\{P(OMe)_3\}(\eta\text{-}C_5H_5)][BF_4]$ **25**. Although the NMR spectra of these phosphite-substituted complexes showed that only one isomer had been formed the data did not establish whether the $P(OMe)_3$ ligand was *cis* or *trans* to the Mo=C bond. This structural detail and the overall geometry of these complexes was, however, clarified by a single-crystal X-ray diffraction study of complex **23**. The resulting structure is shown in Fig. 7 and selected bond lengths and angles are listed in Table 9.

Significantly, although the *anti*-supine $\eta^4(5e)$ geometry is retained, the displacement of MeCN or H_2O by $P(OMe)_3$ leads to a change in stereochemistry, the phosphite ligand now occupying a position *cis* to the molybdenum to carbon double bond. As might be expected comparison (see Tables 5 and 6) of the structural parameters of **23** with those found for **11**, **14** and **18** shows changes in the C(3)–C(4) bond lengths, and also in an opening out of the bond angle C(2)–C(3)–C(4).

In view of this change in stereochemistry on replacement of H_2O or MeCN by $P(OMe)_3$ it was obviously interesting to examine the corresponding reactions with the poorer π-acceptor trimethylphosphine. Treatment of the acetonitrile-substituted cation $[Mo\{=C(Et)\text{-}\eta^3\text{-}[C(Et)C(Et)CHEt]\}Br(NCMe)(\eta\text{-}C_5H_5)][BF_4]$ **14** with PMe_3 led to a rapid reaction and the formation of a single isomer of $[Mo\{=C(Et)\text{-}\eta^3\text{-}[C(Et)C(Et)CHEt]\}Br(PMe_3)(\eta\text{-}C_5H_5)][BF_4]$ **26**. Although comparison of the magnitude of the doublet splitting [*J*(PC) 17.4] observed on the Mo=*C*Et resonance of **26a** with that observed [*J*(PC) 23.7] for the trimethyl phosphite complex **25** suggested a similar *cis* stereochemistry, the absence at this stage of comparative NMR data required structural clarification by single-crystal X-ray crystallography. This established the molecular structure of the cation present in **26a**, which is shown

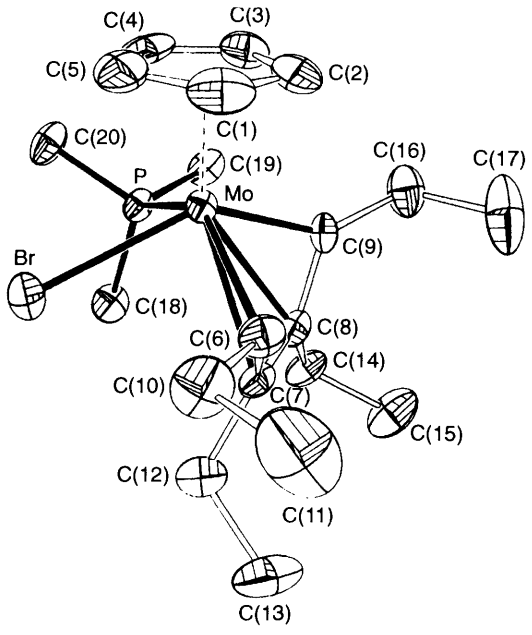

Fig. 8 Molecular structure of the cation present in $[Mo=\{C(Et)\text{-}\eta^3\text{-}[C(Et)C(Et)CHEt]\}Br(PMe_3)(\eta\text{-}C_5H_5)][BF_4]$ **26a**. Ellipsoids are drawn at the 30% probability level

Table 10 Selected bond lengths (Å) and angles (°) for complex **26a**

Br–Mo	2.642(4)	C(6)–Mo	2.331(10)
P–Mo	2.542(5)	C(7)–Mo	2.457(9)
C(7)–C(6)	1.43(1)	C(8)–Mo	2.341(9)
C(8)–C(7)	1.40(1)	C(9)–Mo	1.930(9)
C(9)–C(8)	1.43(1)		
P–Mo–Br	77.4(2)	C(10)–C(6)–C(7)	125.1(9)
C(14)–C(8)–C(7)	123.0(8)	C(8)–C(7)–C(6)	118.1(8)
C(16)–C(9)–C(8)	127.5(8)	C(9)–C(8)–C(7)	117.7(8)

in Fig. 8, selected bond lengths and angles being listed in Table 10. Thus, replacement of acetonitrile by PMe_3 also leads to a change in stereochemistry, the phosphine ligand occupying a position *cis* to the Mo=C bond. As before the *anti*-supine geometry is retained there being variations (see Tables 5 and 6) in the structural parameters of the cisoid $\eta^4(5e)$-butadienyl ligand.

In contrast to this stereochemically clean reaction, treatment of the aqua complex $[Mo\{=C(Et)\text{-}\eta^3\text{-}[C(Et)C(Et)CHEt]\}Br(OH_2)(\eta\text{-}C_5H_5)][BF_4]$ **11** with PMe_3 led to the formation of a mixture (6:1) of two isomers **26a** and **26b**, the major product being that formed from the acetonitrile-substitution reaction. Examination of the NMR spectra for minor isomer **26b** showed that the PMe_3 occupies a position *trans* to the Mo=C bond. When the aqua complex $[Mo\{=C(Me)\text{-}\eta^3\text{-}[C(Me)C(Me)CHMe]\}Cl(OH_2)(\eta\text{-}C_5H_5)][BF_4]$ **9** was treated with trimethylphosphine there was again a lack of stereochemical control, the two isomers (6:1 mixture) **27a** and **27b** being formed. Interestingly, however, the minor isomer **27b** now showed a large *J*(PC) coupling (**27a** 16.0, **27b** 20.0 Hz) with the Mo=C carbon atom suggesting that with the aqua methyl substituted $\eta^4(5e)$-butadienyl system the PMe_3 prefers to adopt a position *trans* to the Mo=C bond.

A rationale for these stereochemical findings clearly requires a detailed understanding of the mechanisms of the individual substitution reactions, but in the absence of such studies it is reasonable to only list the possible reaction pathways. These are (*i*) dissociative loss of H_2O or MeCN followed by capture of the resulting 16e species, (*ii*) a process where the reacting ligand is accommodated by a switch in the bonding mode of the butadienyl ligand, *i.e.* $\eta^4(5e) \longrightarrow \eta^3(3e)$ or $\eta^4(5e)$-butadienyl to

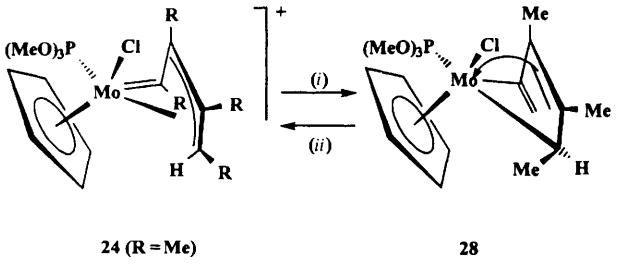

24 (R = Me) 28

Scheme 5 (*i*) $+Li[N(SiMe_3)_2]$; (*ii*) $HBF_4 \cdot Et_2O$

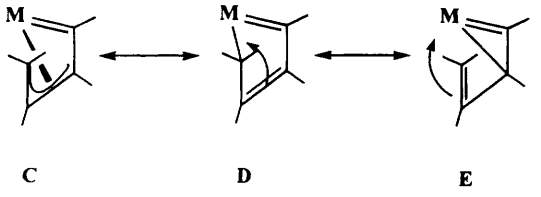

C D E

η^2(3e)-vinyl, this being followed by dissociative loss of H_2O or MeCN.

The three canonical forms **C**, **D** and **E** have been used to describe the bonding in η^4(5e)-butadienyl complexes, and it is therefore interesting to briefly comment on the structural data available for the range of molybdenum complexes described in this paper. Although the ^{13}C NMR data listed in Table 3 shows small variations there is a consistent pattern, and it is difficult to reconcile a variation with increased importance of particular canonical forms. By contrast, in the solid state (Tables 5 and 6) the most significant change in bond parameters is in the case of complex **23**, where there is a strong π-acceptor ligand (trimethylphosphite) suggesting, in view of the shorter C(3)–C(4) bond distance, that there is an increased importance of forms **C** and **E**.

Attention was next turned to a study of the reactivity of the cisoid η^4(5e)-butadienyl ligand, in particular the chemistry of the readily accessible trimethyl phosphite-substituted cations. It was observed (^1H NMR) that addition of NEt_3 to a solution of $[Mo\{=C(Me)\text{-}\eta^3\text{-}[C(Me)C(Me)CHMe]\}Cl\{P(OMe)_3\}(\eta\text{-}C_5H_5)][BF_4]$ **24** in $(CD_3)_2CO$ resulted in selective deuteriation of the Mo=C(*Me*) methyl group. This suggested that irreversible deprotonation of this cationic complex might lead to an interesting new reaction. Indeed addition (−78 °C) of $Li[N(SiMe_3)_2]$ to a stirred suspension of **24** in tetrahydrofuran led to a rapid change from orange to purple, and work-up by low-temperature crystallisation from pentane afforded (52% yield) air-sensitive purple crystals of the neutral complex **28**. Elemental analysis, FAB MS, and examination of the ^1H, $^{13}C\text{-}\{^1H\}$ and $^{31}P\text{-}\{^1H\}$ NMR spectra suggested that the purple complex had the molecular formula $[MoCl\{\eta^4\text{-}CH(Me)=C(Me)\text{-}C(Me)=C=CH_2\}\{P(OMe)_3\}(\eta\text{-}C_5H_5)]$ (see Scheme 5). This was confirmed by a single-crystal X-ray diffraction study. The resultant molecular structure is illustrated in Fig. 9, selected bond lengths and angles are listed in Table 11. Thus the complex contains a $MoCl\{P(OMe)_3\}(\eta\text{-}C_5H_5)$ fragment bonded to an organic molecule which can be viewed as a η^4-bonded vinylallene. This adopts an *endo* conformation, the chlorine atom being *trans* to the $C=CH_2$ group.

In contrast to the related η^4-vinylketene complexes there have been relatively few X-ray crystallographic studies of complexes containing η^4-vinylallene ligands. In our own work we have reported[21] on the structure of $[MoI\{\eta^4\text{-}CH_2=CHC(Me)=C=O\}(CO)(\eta\text{-}C_5Me_5)]$, and it was obviously of interest to compare the bond parameters of the η^4-vinylketene ligand with those of the η^4-vinylallene present in complex **28**. Since both complexes contain a MoX(L)(η-cyclopentadienyl) fragment, in which the C=Y (Y = O or CH_2) carbon is *trans* to a Mo–X bond, such a comparison (see Table 12) is relevant. In both cases M–C^1 is considerably shorter than the other metal–ligand distances suggesting that C^1 participates more strongly

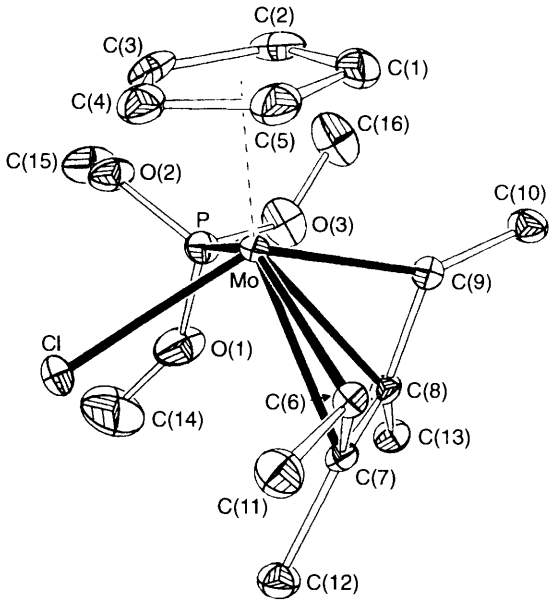

Fig. 9 Molecular structure of $[MoCl\{\eta^4\text{-}CH(Me)=C(Me)\text{-}C(Me)=C=CH_2\}\{P(OMe)_3\}(\eta\text{-}C_5H_5)]$ **28**. Ellipsoids are drawn at the 30% probability level

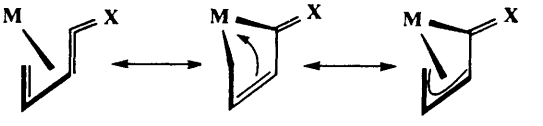

F G H

Table 11 Selected bond lengths (Å) and angles (°) for complex **28**

P–Mo	2.446(4)	C(6)–Mo	2.313(9)
Cl–Mo	2.523(5)	C(7)–Mo	2.437(9)
C(7)–C(6)	1.45(1)	C(8)–Mo	2.380(9)
C(8)–C(7)	1.40(1)	C(9)–Mo	2.106(9)
C(9)–C(8)	1.43(1)		
Cl–Mo–P	83.8(2)	C(9)–C(8)–C(7)	115.3(7)
C(11)–C(6)–C(7)	121.2(7)	C(10)–C(9)–C(8)	130.5(7)
C(8)–C(7)–C(6)	116.8(7)		

in metal–ligand backbonding than the other three carbons of the η^4-system, which all show similar longer bond distances to the metal. The vinylketene and vinyallene moieties are almost planar (C^1–C^2–C^3–C^4, −3.9 and −3.6° respectively) with the cumulated double bond showing an identical [130.5(8) and 130.5(7)°] deviation from linearity. The Y-substituent, *i.e.* O or CH_2, lies out of the C^1–C^2–C^3–C^4 plane in both systems this being reflected in the dihedral angles C^3–C^2–C^1–Y (−134.5 and 127.6°). However, despite these common structural features there is a significant difference in the bonding modes adopted by the η^4-vinylketene and η^4-vinylallene ligands. This can be understood in terms of the canonical representations **F**, **G** and **H**, and is highlighted by the carbon–carbon distances within the respective ligands. Whereas the short C^2–C^3 distance in both systems is accommodated by contributions from the canonical forms **G** and **H**, the presence of a longer [1.45(1) compared with 1.41(1) Å] C^3–C^4 bond in the η^4-vinylallene system implies that in this case there is a more important contribution from **G**, *i.e.* the molybdenacyclocyclopent-3-ene form. By comparison, it is interesting that in a recent report[22] on the molecular structures of the *endo* and *exo* isomers of the η^4-vinylallene complex $[RhCl(PPh_3)\{\eta^4\text{-}CH(SiMe_3)=C(Ph)CH=C=CMe_2\}]$, it was concluded that there was also a major contribution from a

Table 12 X-Ray crystallographic data (bond lengths in Å, angles in °) for [MoI{η⁴-CH_2=CHC(Me)=C=O}(CO)(η-C_5Me_5)] and complex **28**

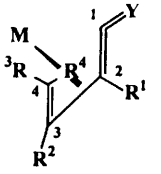

M	Y	R^1	R^2	R^3	R^4	M–C^1	M–C^2	M–C^3	M–C^4	C^1–C^2	C^2–C^3	C^3–C^4	C^1–Y
MoI(CO)(η-C_5Me_5)[a]	O	Me	H	H	H	2.082(8)	2.377(8)	2.414(8)	2.327(7)	1.463(11)	1.409(12)	1.409(12)	1.205(10)
MoCl{P(OMe)$_3$}(η-C_5H_5)[b]	CH_2	Me	Me	Me	H	2.106(9)	2.380(9)	2.437(8)	2.313(9)	1.433(11)	1.404(11)	1.450(11)	1.341(11)

[a] Angles C^1–C^2–C^3–C^4, −3.9; C^2–C^1–Y, 130.5(8); C^3–C^2–C^1–Y, −134.5. [b] Angles C^1–C^2–C^3–C^4, −3.6; C^2–C^1–Y, 130.5(7); C^3–C^2–C^1–Y, −127.6.

Table 13 Charge densities (atomic units) on the η⁴-vinylallene ligand present in complex **28**

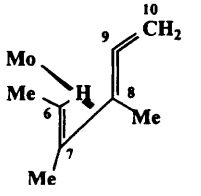

Atom	Net charge
C(6)	−0.3796
C(7)	−0.0321
C(8)	−0.1296
C(9)	−0.4041
C(10)	−0.3914

Table 14 Charge densities (atomic units) and p-orbital coefficients for the cisoid η⁴(5e)-butadienyl ligand present in complex **23**

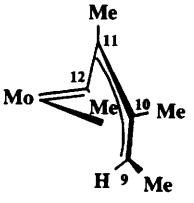

		p-Orbital coefficient		
Atom	Net charge	p_x	p_y	p_z
C(9)	−0.131	+0.0337	−0.0719	+0.0292
C(10)	+0.107	−0.1192	−0.0685	−0.0812
C(11)	+0.096	+0.0057	+0.1516	−0.0345
C(12)	−0.105	+0.0696	+0.6223	+0.1339

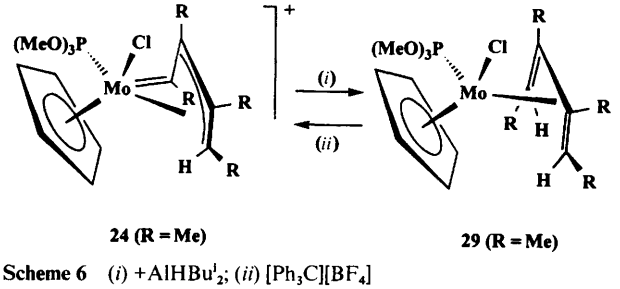

24 (R = Me) **29 (R = Me)**

Scheme 6 (*i*) +AlHBu$^i_2$; (*ii*) [Ph_3C][BF_4]

rhodacyclopent-3-ene canonical form. Conversely, the slightly shorter [1.433(11) *cf.* 1.463(11) Å] C^1–C^2 distance in the η⁴-vinylketene species is consistent with a more significant contribution from canonical form **H**.

The formation of the η⁴-vinylallene complex [MoCl{η⁴-CH(Me)=C(Me)C(Me)=CCH_2}{P(OMe)$_3$}(η-C_5H_5)] **28** by deprotonation of the η⁴(5e)-butadienyl substituted cation [Mo{=C(Me)-η³-[C(Me)C(Me)CHMe]}Cl{P(OMe)$_3$}(η-C_5H_5)][BF_4] **24** was especially interesting because previously such species had been synthesised either by reaction of a vinylallene with a suitable metal complex,[23] or by a Wadsworth–Emmons reaction (C=C=O ⟶ C=C=$CHCO_2Bu^t$) on the corresponding η⁴-vinylketene complex.[24] It was clearly interesting to explore whether the reaction **24** ⟶ **28** could be reversed, and in order to assess this possibility an EHMO calculation was carried out using the molecular parameters established by X-ray crystallography for **28**. Since it must be expected that a protonation reaction would be charge controlled, the charge density on the carbon atoms of the η⁴-vinylallene moiety was computed. As shown in Table 13 there is an appreciable negative charge on carbon atoms C(6), C(9) and C(10) (crystallographic numbering). When complex **28** was reacted with HBF_4·Et_2O at −78 °C in dichloromethane a proton was delivered selectively to C(10), *i.e.* the end carbon of the methylene group, regenerating the cisoid η⁴(5e)-butadienyl complex **24** in high yield (95%), suggesting that the bulk of the reagent, [Et_2OH][BF_4], which delivers the proton is also a factor in controlling the site of attack. The establishment of an interrelationship between η⁴(5e)-butadienyl and η⁴-vinylallene ligands is potentially important, suggesting a possible general route to cisoid η⁴(5e)-butadienyl complexes *via* the protonation of η⁴-vinylallene complexes.

Returning to the more general question of the potential reactivity of the phosphite-substituted cations towards nucleophilic reagents, an EHMO calculation using the molecular parameters derived from the X-ray crystallographic study with complex **23** established the charge density distribution and p-orbital coefficients for the carbon atoms of the η⁴(5e)-butadienyl ligand, listed in Table 14. These data clearly indicated that nucleophilic attack should occur under frontier orbital control on the Mo=C π* orbital lying orthogonal to the metal–carbon vector. However, when attempts were made to react **23** or **24** with BH_4^-, $BHBu^s_3^-$ or $BHEt_3^-$, it was observed that deprotonation competed with the delivery of 'H^-' to the Mo=C carbon atom. Alternative sources of 'H^-' were therefore explored. It was found[25] that reaction of **23** with AlHBu$^i_2$ in tetrahydrofuran led to the selective formation (76% yield) of the purple, air-sensitive crystalline η⁴-bonded 1,3-diene complex **29** (see Scheme 6) which was characterised by elemental analysis, FAB MS, ^{1}H, ^{13}C-{^{1}H} and ^{31}P-{^{1}H} NMR spectroscopy. Nuclear Overhauser enhancement (NOE) experiments involving the two diene CHMe groups confirmed that the C*H*Me protons are both on the inside of the 1,3-diene in agreement with selective delivery of 'H^-' to the Mo=C carbon. It was assumed that the 1,3-diene adopts the illustrated *endo*-conformation, which is supported by a preliminary study of the corresponding η⁵-indenyl substituted system, where it was observed that the C*H*Me 1,3-diene protons shifted to δ −0.56 and −1.63.

It was further found that this 1,3-diene complex can be reconverted into the parent η⁴(5e)-butadienyl complex (see Scheme 6). Addition of [Ph_3C][BF_4] to a dichloromethane solution of **29** at −78 °C resulted in a rapid change from purple to

orange and on addition of diethyl ether orange crystals of **23** were precipitated in 68% yield. This reaction is most unusual and involves an unprecedented formal hydride abstraction of the C–H bond of a η^4-bonded 1,3-diene *trans* to a bromo ligand. It is interesting that the reaction of Ph_3C^+ with $[WMe_2(\eta\text{-}C_5H_5)_2]$ has been previously[26] shown to occur *via* electron transfer followed by $H^\bullet$ abstraction by the trityl radical to form the cation $[W(=CH_2)Me(\eta\text{-}C_5H_5)_2]^+$. This suggests that the reaction of **29** with $[Ph_3C][BF_4]$ involves the formation of a 17e radical cation which then undergoes a hydrogen ($H^\bullet$) abstraction reaction by the trityl radical, which is facilitated by spin delocalisation *via* the developing Mo=C bond. The reason for the regioselectivity in this formal hydride abstraction reaction is not clear.

In conclusion, the protonation of halogenobis(alkyne) complexes has been shown to provide a new stereoselective synthetic entry point to a range of cationic molybdenum η^4(5e)-butadienyl substituted complexes. These cations have been shown to undergo stereoselective substitution reactions, reversible deprotonation to form a η^4-vinylallene complex, and nucleophilic attack on the carbene carbon to form a η^4-1,3-diene complex, which on treatment with trityl cation undergoes an unusual hydride abstraction reaction to reform stereoselectively the parent cationic η^4(5e)-butadienyl complex.

Experimental

All reactions were carried out under an atmosphere of dry, oxygen-free dinitrogen, using standard Schlenk techniques. Solvents were freshly distilled over an appropriate drying agent and further degassed before use where necessary. Column chromatography was performed using BDH alumina, Brockmann activity II. The ^1H, ^{13}C-{^1H}, ^{31}P-{^1H} and ^{19}F NMR spectra were recorded on Bruker AM360, and JEOL GX 270 and EX400 spectrometers. Data are given for room-temperature measurements unless otherwise stated. Chemical shifts are positive to high frequency of the reference $SiMe_4$ for ^{13}C and ^1H, H_3PO_4 (85%, external) for ^{31}P and CCl_3F (external) for ^{19}F. Infrared spectra were recorded on a Nicolet 510P FT-IR spectrometer.

Preparations

$[MoCl(\eta^2\text{-}EtC_2Et)_2(\eta\text{-}C_5H_5)]$ 4. A solution of $[Mo(NCMe)(\eta^2\text{-}EtC_2Et)_2(\eta\text{-}C_5H_5)][BF_4]$[27] (0.25 g, 0.55 mmol) and anhydrous LiCl (0.035 g, 0.83 mmol) in tetrahydrofuran (10 cm^3) was heated under reflux for 1 h. The solution was allowed to cool to room temperature and the volatiles removed *in vacuo*. The residue was dissolved in CH_2Cl_2 (2 cm^3) and chromatographed. Elution with Et_2O gave a bright yellow band, which was collected and recrystallised from Et_2O–hexane to give orange-red *crystals* of **4** (0.11 g, 56%) (Found: C, 56.4; H, 7.0. $C_{17}H_{25}ClMo$ requires C, 56.6; H, 7.0%). NMR (CD_2Cl_2): ^1H, δ 5.37 (s, 5 H, C_5H_5), 3.17–2.98 (br m, 8 H, $4CH_2$), 1.36–0.83 (br, 12 H, 4Me); ^{13}C-{H}, δ 184.6 (Et*C*≡), 173.2 (Et*C*≡), 101.3 (C_5H_5), 3.03 (CH_2), 22.0 (CH_2), 13.8 (Me).

A similar procedure was used for the synthesis of $[MoCl(\eta^2\text{-}MeC_2Me)_2(\eta\text{-}C_5H_5)]$ **1** (57%) (Found: C, 51.2; H, 5.7. $C_{13}H_{17}ClMo$ requires C, 51.3; H, 5.6%), NMR ($CDCl_3$): ^1H, δ 5.37 (s, 5 H, C_5H_5), 2.65 (s, 12 H, Me), ^{13}C-{^1H}, δ 180.1 (Me*C*≡), 169.0 (Me*C*≡), 100.9 (C_5H_5), 15.8 (Me); $[MoBr(\eta^2\text{-}MeC_2Me)_2(\eta\text{-}C_5H_5)]$ **2** (48%) (Found: C, 44.2; H, 4.9. $C_{13}H_{17}BrMo$ requires C, 44.7; H, 4.9%), NMR ($CDCl_3$): ^1H, δ 5.40 (s, 5 H, C_5H_5), 2.69 (s, 12 H, Me), ^{13}C-{^1H}(253 K), δ 179.7 (Me*C*≡), 164.3 (Me*C*≡), 100.5 (C_5H_5), 20.2 (*Me*C≡), 15.6 (*Me*C≡); $[MoI(\eta^2\text{-}MeC_2Me)_2(\eta\text{-}C_5H_5)]$ **3** (61%) (Found: C, 39.5; H, 4.3. $C_{13}H_{17}IMo$ requires C, 39.4; H, 4.3%), NMR ($CDCl_3$): ^1H, δ 5.39 (s, 5 H, C_5H_5), 2.77 (br, s, 12 H, Me), ^{13}C-{^1H}(243 K), δ 178.2 (Me*C*≡), 160.5 (Me*C*≡), 99.8 (C_5H_5), 20.9 (*Me*C≡), 19.7 (*Me*C≡); $[MoBr(\eta^2\text{-}EtC_2Et)_2(\eta\text{-}C_5H_5)]$ **5** (62%) (Found: C, 49.7; H, 6.3. $C_{17}H_{25}BrMo$ requires C, 50.3; H, 6.2%), NMR (CD_2Cl_2): ^1H, δ 5.38 (s, 5 H, C_5H_5), 3.25–2.98 (br m, 8 H, $4CH_2$), 1.26–0.88 (br, m, 12 H, 4Me), ^{13}C-{^1H}, δ 183.7 (Et*C*≡), 171.1 (Et*C*≡), 101.3 (C_5H_5), 30.5 (CH_2), 24.6 (CH_2), 14.1 (Me); $[MoI(\eta^2\text{-}EtC_2Et)_2(\eta\text{-}C_5H_5)]$ **6** (48%) (Found: C, 44.9; H, 5.4. $C_{17}H_{25}IMo$ requires C, 45.2; H, 5.6%), NMR (CD_2Cl_2): ^1H, δ 5.40 (s, 5 H, C_5H_5), 3.35–3.12 (br m, 8 H, $4CH_2$), 1.37–0.84 (br m, 12 H, 4Me), ^{13}C-{^1H}, δ 181.9 (Et*C*≡), 166.5 (Et*C*≡), 100.2 (C_5H_5), 29.6 (CH_2), 13.9 (Me); $[MoBr(\eta^2\text{-}MeC_2Me)_2(\eta^5\text{-}C_9H_7)]$ **7** (58%) (Found: C, 51.0; H, 4.7. $C_{17}H_{19}BrMo$ requires C, 51.2; H, 4.8%), NMR ($CDCl_3$): ^1H, δ 7.36 (m, 2 H, C_9H_7), 7.10–6.95 (m, 2 H, C_9H_7), 6.09 [d, 2 H, C_9H_7, *J*(HH) 3.3], 5.52 [t, 1 H, C_9H_7, *J*(HH) 3.3 Hz], 2.55 (s, 12 H, Me), ^{13}C-{^1H}(243 K), δ 180.3 (Me*C*≡), 167.7 (Me*C*≡), 126.2, 122.9, 122.1, 109.3, 85.1 (C_9H_7), 18.9 (*Me*C≡), 14.6 (*Me*C≡); $[MoBr(\eta^2\text{-}EtC_2Et)_2(\eta^5\text{-}C_9H_7)]$ **8** (65%) (Found: C, 55.2; H, 6.1. $C_{21}H_{27}BrMo$ requires C, 55.4; H, 6.0%), NMR (CD_2Cl_2): ^1H, δ 7.27 [dd, 2 H, C_9H_7, *J*(HH), 3.1, 6.3], 7.00 [dd, 2 H, C_9H_7, *J*(HH) 3.1, 6.3], 6.12 [d, 2 H, C_9H_7, *J*(HH) 3.3], 5.66 [t, 1 H, C_9H_7, *J*(HH) 4.2 Hz], 3.00 (br m, 8 H, $4CH_2$), 1.00 (br m, 12 H, 4Me), ^{13}C-{^1H}, δ 184.0 (Et*C*≡), 175.5 (Et*C*≡), 138.2, 126.7, 123.8, 110.5, 85.9 (C_9H_7), 22.4 (CH_2) 14.5 (Me).

$[Mo\{=C(Me)\text{-}\eta^3\text{-}[C(Me)C(Me)CHMe]\}Cl(OH_2)(\eta\text{-}C_5H_5)][BF_4]$ 9. Complex **1** (1.05 g, 3.45 mmol) was dissolved in CH_2Cl_2 (15 cm^3), cooled to −78 °C and $HBF_4{\cdot}Et_2O$ (597 μl, 4.03 mmol) was added dropwise to the solution, resulting in a change from yellow to purple. The solution was allowed to warm to room temperature over 2 h, filtered through Celite and the volatiles removed *in vacuo*. The residue was recrystallised from CH_2Cl_2–pentane to give red *crystals* of **9** (0.98 g, 70%) (Found: C, 38.2; H, 4.9. $C_{13}H_{20}BClF_4MoO$ requires C, 38.0; H, 4.9%). NMR (CD_3NO_2): ^1H, δ 6.03 (s, 5 H, C_5H_5), 4.06 (br s, 2 H, H_2O), 2.92 (br s, 3 H, Mo=CMe), 2.21 (br m, 4 H, Me, C*H*Me), 2.07 (br s, 6 H, 2CMe); ^{13}C-{^1H}, δ 306.6 (Mo=*C*Me), 135.6 (*C*Me), 115.1 (*C*Me), 104.6 (C_5H_5), 73.8 (*C*HMe), 28.1, 16.5, 16.0, 11.4 (Me). Mass spectra, *m/z*: FAB(+), $[M - H_2O]^+$ 307; FAB(−), BF_4^- 87.0.

$[Mo\{=C(Et)\text{-}\eta^3\text{-}[C(Et)C(Et)CHEt]\}Cl(OH_2)(\eta\text{-}C_5H_5)][BF_4]$ 10. Complex **4** (0.186 g, 0.52 mmol) was dissolved in dichloromethane (5 cm^3), cooled to −78 °C and $HBF_4{\cdot}Et_2O$ (77 μl, 0.52 mmol) was added dropwise with stirring. The reaction mixture changed from orange-red to cherry red. The solution was allowed to warm to room temperature over 2 h and then filtered through Celite. The volatiles were removed *in vacuo*, the product dissolved in CH_2Cl_2 (5 cm^3) and then precipitated with Et_2O (15 cm^3). Recrystallisation (0 °C) from CH_2Cl_2–pentane gave purple *crystals* of **10** (0.163 g, 70%) (Found: C, 43.3; H, 6.1. $C_{17}H_{28}BClF_4MoO$ requires C, 43.7; H, 6.0%). NMR (CD_3NO_2): ^1H, δ 6.05 (s, 5 H, C_5H_5), 3.95 (br s, 2 H, H_2O), 3.36–2.31 (m, 9 H, $4CH_2$, C*H*Et), 1.50 [t, 3 H, Me, *J*(HH) 7.35], 1.49 [t, 3 H, Me, *J*(HH) 7.23], 1.17 [t, 3 H, Me, *J*(HH) 7.5], 0.97 [t, 3 H, Me, *J*(HH) 7.3 Hz]; ^{13}C-{^1H}, δ 303.8 (Mo=*C*Et), 137.6 (*C*Et), 114.9 (*C*Et), 99.3 (C_5H_5), 74.7 (*C*HEt), 32.4, 19.1, 18.7, 16.0 (CH_2), 11.9, 8.9, 8.8, 7.3 (Me).

$[Mo\{=C(Et)\text{-}\eta^3\text{-}[C(Et)C(Et)CHEt]\}Br(OH_2)(\eta\text{-}C_5H_5)][BF_4]$ 11. Similarly, reaction of complex **5** (0.47 g, 1.16 mmol) with $HBF_4{\cdot}Et_2O$ (172 μl, 1.16 mmol) in CH_2Cl_2 (15 cm^3) gave upon recrystallisation from CH_2Cl_2–pentane pink *crystals* of **11** (0.43 g, 75%) (Found: C, 39.7; H, 5.4. $C_{17}H_{28}BBrF_4MoO$ requires C, 39.9; H, 5.5%). NMR (CD_2Cl_2): ^1H, δ 5.98 (s, 5 H, C_5H_5), 4.12 (br s, 2 H, H_2O), 3.12–2.26 (m, 9 H, $4CH_2$, C*H*Et), 1.47 [t, 3 H, Me, *J*(HH) 7.7], 1.46 [t, 3 H, Me, *J*(HH) 7.7], 1.21 [t, 3 H, Me, *J*(HH) 7.2], 0.93 [t, 3 H, Me, *J*(HH) 7.5 Hz]; ^{13}C-{^1H}, δ 298.4 (Mo=*C*Et), 147.8 (*C*Et), 117.9 (*C*Et), 102.8 (C_5H_5), 79.3 (*C*HEt), 37.2, 23.3, 23.0, 21.2 (CH_2), 16.9, 14.4, 13.8, 12.1 (Me); ^{11}B-{^1H}, δ −3.09 (BF_4^-); ^{19}F, δ −150.77 (br s, BF_4) (^{10}B iso-

topomer appeared as a shoulder). Mass spectra, *m/z*: FAB(+), $[M - H_2O]^+$ 406.9; FAB(−), BF_4^- 87.0.

[Mo{=C(Et)-η³-[C(Et)C(Et)CHEt]}I(OH₂)(η-C₅H₅)][BF₄] 12. In the same way, reaction of complex **6** (0.21 g, 0.47 mmol) with $HBF_4 \cdot Et_2O$ (69 μl, 0.47 mmol) in CH_2Cl_2 (5 cm^3) gave upon recrystallisation from CH_2Cl_2–pentane purple *crystals* of **12** (0.02 g, 78%) (Found: C, 36.5; H, 5.0. $C_{17}H_{28}BIF_4MoO$ requires C, 36.6; H, 5.0%). NMR (CD_3NO_2): ^1H, δ 6.08 (s, 5 H, C_5H_5), 4.13 (br s, 2 H, H_2O), 3.13–2.43 (m, 9 H, $4CH_2$, C*H*Et), 1.67 [t, 3 H, Me, *J*(HH) 7.8], 1.65 [t, 3 H, Me, *J*(HH) 7.7], 1.09 [t, 3 H, Me, *J*(HH) 7.5], 0.97 [t, 3 H, Me, *J*(HH) 7.6 Hz]; ^{13}C-{^1H}, δ 302.2 [Mo=*C*Et], 132.5 (*C*Et), 108.0 (*C*Et), 97.1 (C_5H_5), 7.10 (*C*HEt), 33.4, 21.7, 21.4, 20.0 (CH_2), 11.5, 8.9, 8.8, 6.4 (Me).

[Mo{=C(Me)-η³-[C(Me)C(Me)CHMe]}Br(NCMe)(η-C₅H₅)][BF₄] 13. Reaction of complex **2** (0.50 g, 1.43 mmol) with $HBF_4 \cdot Et_2O$ (200 μl, 1.43 mmol) in CH_2Cl_2 (20 cm^3) at −78 °C gave upon addition of Et_2O (20 cm^3) a salmon red precipitate. This was collected and recrystallised from MeCN–Et_2O to give deep red *crystals* of **13** (0.50 g, 80%) (Found: C, 37.4; H, 4.5; N, 2.5. $C_{15}H_{21}BBrF_4MoN$ requires C, 37.7; H, 4.4; N, 2.9%). IR (CH_2Cl_2): ν(NC) 2294 cm^{-1}. NMR (CD_3NO_2): ^1H, δ 6.03 (s, 5 H, C_5H_5), 2.78 (s, 3 H, Mo=CMe), 2.37 (s, 3 H, MeCN), 2.29 (m, 1 H, C*H*Me), 2.15 (s, 3 H, CMe), 2.04 [d, 3 H, CH*Me*, *J*(HH) 6.0 Hz]; ^{13}C-{^1H}, δ 297.3 (Mo=*C*Me), 140.7 (*C*Me), 134.8 (Me*C*N), 120.1 (*C*Me), 104.0 (C_5H_5), 74.4 (*C*HMe), 28.6, 16.3, 15.9, 12.3 (Me).

[Mo{=C(Et)-η³-[C(Et)C(Et)CHEt]}Br(NCMe)(η-C₅H₅)][BF₄] 14. Complex **11** (0.14 g, 0.29 mmol) was dissolved in MeCN (10 cm^3) and stirred at room temperature for 1 h. The volatiles were removed *in vacuo* and the residue dissolved in CH_2Cl_2 (3 cm^3) and the solution filtered through a Celite plug. Addition of diethyl ether (10 cm^3) gave an orange-red precipitate. This was collected and crystallised by MeCN–Et_2O layer diffusion at room temperature to give bright orange *crystals* of **14** (0.13 g, 89%) (Found: C, 42.6; H, 5.4. $C_{19}H_9BBrF_4MoN$ requires C, 42.7; H, 5.5%). IR(CH_2Cl_2): ν(NC) 2295 cm^{-1}. NMR (CD_2Cl_2): ^1H, δ 6.04 (s, 5 H, C_5H_5), 3.18–2.52 (m, 6 H, $3CH_2$), 2.37 (s, 3 H, MeCN), 2.26 (m, 3 H, CH_2, C*H*Et), 1.51 [t, 3 H, Me, *J*(HH) 7.7], 1.49 [t, 3 H, Me, *J*(HH) 7.8], 1.27 [t, 3 H, Me, *J*(HH) 7.5], 1.02 [t, 3 H, Me, *J*(HH) 7.5 Hz]; ^{13}C-{^1H}, δ 297.4 (Mo=*C*Et), 140.2 (*C*Et), 134.1 (Me*C*N), 119.3 (*C*Et), 102.5 (C_5H_5), 79.5 (*C*HEt), 37.6, 24.4, 23.4, 20.8 (CH_2), 16.7, 14.3, 14.2, 12.0 (Me), 4.1 (*Me*CN). Mass spectra, *m/z*: FAB(+), $[M - MeCN]^+$ 407.0; FAB(−), BF_4^- 87.0.

[Mo{=C(Et)-η³-[C(Et)C(Et)CHEt]}I(NCMe)(η-C₅H₅)][BF₄] 15. A solution of complex **12** (0.38 g, 0.68 mmol) in MeCN (20 cm^3) was stirred at room temperature for 2 h to give, in a similar way, dark red-brown *crystals* of **15** (0.37 g, 93%) (Found: C, 39.3; H, 5.1; N, 2.4. $C_{19}H_{29}BF_4IMoN$ requires C, 39.3; H, 5.0; N, 2.4%). NMR (CD_3NO_2): ^1H, δ 6.02 (s, 5 H, C_5H_5), 3.30–2.51 (m, 8 H, $4CH_2$), 2.47 (s, 3 H, MeCN), 2.27 (m, 1 H, C*H*Et), 1.54 [t, 3 H, Me, *J*(HH) 7.7], 1.47 [t, 3 H, Me, *J*(HH) 7.7], 1.21 [t, 3 H, Me, *J*(HH) 7.4], 0.96 [t, 3 H, Me, *J*(HH) 7.5 Hz]; ^{13}C-{^1H}, δ 301.3 (Mo=*C*Et), 137.0 (*C*Et), 133.2 (Me*C*N), 118.8 (*C*Et), 101.9 (C_5H_5), 75.8 (*C*HEt), 38.2, 24.7, 24.3, 24.1 (CH_2), 16.4, 15.7, 14.4, 11.4 (Me), 3.66 (*Me*CN). Mass spectra, *m/z*: FAB(+), $[M]^+$ 494.0, $[M - MeCN]^+$ 454.9; FAB(−), BF_4^- 87.0.

[Mo{=C(Me)-η³-[C(Me)C(Me)CHMe]}Cl₂(η-C₅H₅)] 16. A solution of anhydrous LiCl (0.02 g, 0.45 mmol) in thf (10 cm^3) was added with stirring at room temperature to a solution of complex **9** (0.19 g, 0.30 mmol) in CH_2Cl_2 (10 cm^3). The solution changed from orange to purple. The volatiles were removed *in vacuo*, the residue extracted into CH_2Cl_2 (20 cm^3) and filtered through Celite. Reduction of the volume of the solvent and addition of hexane gave purple *crystals* of **16** (0.17 g, 78%) (Found: C, 45.8; H, 5.2. $C_{13}H_{18}Cl_2Mo$ requires C, 45.8; H, 5.3%). NMR (CD_2Cl_2): ^1H, δ 5.70 (s, 5 H, C_5H_5), 2.80 (s, 3 H, Mo=C*Me*), 2.08 (br s, 6 H, 2CMe), 2.03 [d, 3 H, CH*Me*, *J*(HH) 6.1], 1.90 [q, 1 H, C*H*Me, *J*(HH) 6.1]; ^{13}C-{^1H}, δ 291.3 (Mo=*C*Me), 134.2 (*C*Me), 113.6 (*C*Me), 102.6 (C_5H_5), 70.0 (*C*HMe), 27.5, 16.8, 16.4, 11.1 (Me). Mass spectrum, *m/z*: FAB(+), $[M]^+$ 341, $[M - Cl]^+$ 306.

[Mo{=C(Et)-η³-[C(Et)C(Et)CHEt]}Cl₂(η-C₅H₅)] 17. A solution of anhydrous LiCl (0.02 g, 0.45 mmol) in CH_2Cl_2–thf (1 : 1, 5 cm^3) was added dropwise with stirring to a solution of complex **10** (0.14 g, 0.30 mmol) in the same solvent system (10 cm^3). There was an immediate deepening in colour, and after 30 min the volatiles were removed *in vacuo* from the deep red solution. The residue was dissolved in CH_2Cl_2 (10 cm^3) and filtered through a Celite plug. The solvent was removed and the residue crystallised from CH_2Cl_2–Et_2O–pentane by layer diffusion to give wine red *crystals* of **17** (0.10 g, 86%) (Found: C, 50.9; H, 6.6. $C_{17}H_{26}Cl_2Mo$ requires C, 51.4; H, 6.6%). NMR (CD_2Cl_2): ^1H, δ 5.74 (s, 5 H, C_5H_5), 3.25 (m, 2 H, CH_2), 2.56 (m, 2 H, CH_2), 2.49 [q, 2 H, CH_2, *J*(HH) 7.7], 2.25 (m, 2 H, CH_2), 1.96 [tq, 1 H, C*H*Et, *J*(HH) 8.16, *J*(HH) 3.6], 1.39 [t, 3 H, Me, *J*(HH) 7.7], 1.37 [t, 3 H, Me, *J*(HH) 7.7], 1.08 [t, 3 H, Me, *J*(HH) 7.5], 0.95 [t, 3 H, Me, *J*(HH) 7.5]; ^{13}C-{^1H}, δ 294.3 (Mo=*C*Et), 138.5 (*C*Et), 116.1 (*C*Et), 102.3 (C_5H_5), 76.1 (*C*HEt), 36.1, 24.1, 23.6, 20.0 (CH_2), 16.8, 14.1, 14.0, 12.8 (Me).

[Mo{=C(Et)-η³-[C(Et)C(Et)CHEt]}Br₂(η-C₅H₅)] 18. Similarly, reaction of anhydrous lithium bromide (0.03 g, 0.36 mmol) with **11** (0.12 g, 0.24 mmol) in CH_2Cl_2–thf (1 : 1, 15 cm^3) afforded upon crystallisation from CH_2Cl_2–Et_2O–pentane pink-red *crystals* of **18** (0.09 g, 73%) (Found: C, 41.7; H, 5.2. $C_{17}H_{26}Br_2Mo$ requires C, 42.0; H, 5.4%). NMR (CD_2Cl_2): ^1H, δ 5.75 (s, 5 H, C_5H_5), 3.24 [dq, 1 H, CH(*H*), *J*(HH), 14.7, *J*(HH) 7.2], 2.90 [dq, 1 H, C*H*(H), *J*(HH) 14.6, *J*(HH) 7.6], 2.64 (m, 4 H, $2CH_2$), 2.41 [dq, 1 H, CH(*H*), *J*(HH) 14.3, *J*(HH) 7.5], 2.25 [dq, 1 H, C*H*(H), *J*(HH) 1.41, *J*(HH) 7.0], 2.09 [d, 1 H, C*H*Et, *J*(HH) 3.4], 1.39 [t, 6 H, 2Me, *J*(HH) 7.7], 1.08 [t, 3 H, Me, *J*(HH) 7.5], 0.94 [t, 3 H, Me, *J*(HH) 7.5 Hz]; ^{13}C-{^1H}, δ 295.3 (Mo=*C*Et), 136.7 (*C*Et), 113.8 (*C*Et), 101.5 (C_5H_5), 74.5 (*C*HEt), 36.6, 25.3, 24.2, 20.7 (CH_2), 16.8, 14.7, 14.5, 11.8 (Me).

[Mo{=C(Et)-η³-[C(Et)C(Et)CHEt]}I₂(η-C₅H₅)] 19. Reaction of anhydrous lithium iodide (0.05 g, 0.34 mmol) with complex **12** (0.12 g, 0.23 mmol) in CH_2Cl_2–thf (1 : 1, 10 cm^3) afforded wine red *crystals* of **19** (0.11 g, 82%) (Found: C, 35.1; H, 4.6. $C_{17}H_{26}I_2Mo$ requires C, 35.2; H, 4.5%). NMR (CD_2Cl_2): ^1H, δ 5.80 (s, 5 H, C_5H_5), 3.23 [dq, 1 H, CH(*H*), *J*(HH) 14.4, *J*(HH) 7.8], 3.02 [dq, 1 H, C*H*(H), *J*(HH) 14.4, *J*(HH) 7.8], 2.73 (m, 4 H, $2CH_2$), 2.5 [m, 1 H, C*H*(H)], 2.33 [m, 1 H, CH(*H*)], 2.25 (m, 1 H, C*H*Et), 1.40 [t, 3 H, Me, *J*(HH) 7.7], 1.38 [t, 3 H, Me, *J*(HH) 7.7], 1.10 [t, 3 H, Me, *J*(HH) 7.3], 0.94 [t, 3 H, Me, *J*(HH) 7.8 Hz]; ^{13}C-{^1H}, δ 295.5 (Mo=*C*Et), 134.2 (*C*Et), 110.0 (*C*Et), 99.8 (C_5H_5), 70.6 (*C*HEt), 37.4, 28.0, 26.1, 23.2 (CH_2), 16.9, 16.0, 15.8, 10.7 (Me).

[Mo{=C(Me)-η³-[C(Me)C(Me)CHMe]}Br₂(η-C₅H₅)] 20. Lithium bromide (0.10 g, 1.15 mmol) was added to a solution of complex **13** (0.40 g, 0.92 mmol) in CH_2Cl_2–thf (1 : 1, 20 cm^3). The purple reaction mixture was worked up by the above procedure to give upon recrystallisation from CH_2Cl_2–hexane purple *crystals* of **20** (0.28 g, 72%) (Found: C, 36.0; H, 4.2. $C_{13}H_{18}Br_2Mo$ requires C, 36.3; H, 4.2%). NMR (CD_2Cl_2): ^1H, δ 5.72 (s, 5 H, C_5H_5), 2.60 (s, 3 H, Mo=CMe), 2.25 (s, 3 H, CMe), 2.23 (s, 3 H, CMe), 2.05 (m, 4 H, C*H*Me); ^{13}C-{^1H}, δ 292.6 (Mo=*C*Me), 132.4 (*C*Me), 111.2 (*C*Me), 101.8 (C_5H_5), 68.2 (*C*HMe), 28.2, 17.9, 17.6, 12.2 (Me). Mass spectrum, *m/z*: FAB(+), $[M]^+$ 432.0, $[M - Br]^+$ 350.0.

[Mo{=C(Et)-η³-[C(Et)C(Et)CHEt]}ClI(η-C_5H_5)] 21. A solution of complex **15** (0.10 g, 0.33 mmol) and anhydrous LiCl (0.015 g, 0.35 mmol) in CH_2Cl_2–thf (1:1, 10 cm^3) was stirred at room temperature for 2 h. The volatiles were removed *in vacuo*, the residue extracted with CH_2Cl_2 (2 × 3 cm^3) and the red solution filtered through Celite. The volume of the filtrate was reduced (*ca.* 2 cm^3) and hexane (50 cm^3) added. The resultant precipitate was recrystallised from CH_2Cl_2–Et_2O to give dark red *crystals* of **21** (0.16 g, 97%) (Found: C, 41.7; H. 5.4. $C_{17}H_{26}ClIMo$ requires C, 41.8; H, 5.3%). NMR (CD_2Cl_2): ^1H δ 5.76 (s, 5 H, C_5H_5), 3.16 (m, 9 H, $4CH_2$, C*H*Et), 1.39 [t, 3 H, Me, *J*(HH) 7.7], 1.38 [t, 3 H, Me, *J*(HH) 7.7], 1.14 [t, 3 H, Me, *J*(HH) 7.5], 0.92 [t, 3 H, Me, *J*(HH) 7.5 Hz]; ^{13}C-{^1H}, δ 297.8 (Mo=*C*Et), 135.8 (*C*Et), 114.6 (*C*Et), 100.6 (C_5H_5), 76.0 (*C*HEt), 36.2, 23.8, 23.6, 23.3 (CH_2), 16.4, 16.1, 13.9, 11.8 (Me). Mass spectrum, *m/z*: FAB(+), $[M]^+$ 494.0, $[M - Cl]^+$ 454.9.

Reaction of complex 14 with lithium iodide. Complex **14** (0.44 g, 0.83 mmol) was dissolved in CH_2Cl_2–thf (1:1, 20 cm^3). To this solution was added anhydrous LiI (0.17 g, 1.24 mmol). The reaction mixture was stirred at room temperature for 3 h, and then worked up by the above procedure to give dark purple *crystals* (0.39 g) of a mixture of **19** (major) and [Mo{=C(Et)-η³-[C(Et)C(Et)CHEt]}BrI(η-C_5H_5)] **22** (minor), identified by NMR and mass spectrometry. NMR (CD_2Cl_2) (**22**): ^1H, δ 5.77 (s, 5 H, C_5H_5), 3.27–2.19 (m, 9 H, $4CH_2$, C*H*Et), 1.40 [t, 3 H, Me, *J*(HH) 7.3], 1.38 [t, 3 H, Me, *J*(HH) 7.4], 1.12 [t, 3 H, Me, *J*(HH) 7.3], 0.93 [t, 3 H, Me, *J*(HH) 7.6]; ^{13}C-{^1H}, δ 296.8 (Mo=*C*Et), 133.9 (*C*Et), 112.9 (*C*Et), 110.3 (C_5H_5), 74.0 (*C*HEt), 36.7, 27.9, 23.6, 23.3 (CH_2), 16.4, 16.1, 13.4, 10.8 (Me).

[Mo{=C(Me)-η³-[C(Me)C(Me)CHMe]}Br{P(OMe)₃}(η-C_5H_5)][BF_4] 23. Trimethyl phosphite (0.18 g, 1.45 mmol) was added dropwise with stirring at room temperature to a solution of complex **13** (0.04 g, 0.91 mmol) in CH_2Cl_2 (15 cm^3). The solution became bright orange, and after 10 min the reaction mixture was filtered through Celite, the volume of the solvent was reduced *in vacuo* (to 5 cm^3) and Et_2O (30 cm^3) added. The resultant precipitate was collected and recrystallised from CH_2Cl_2–Et_2O to give orange *crystals* of **23** (0.45 g, 88%) (Found: C, 34.4; H, 4.8. $C_{16}H_{27}BBrF_4MoOP$ requires C, 34.2; H, 4.9%). NMR (CD_2NO_2): ^1H, δ 5.86 [d, 5 H, C_5H_5, *J*(PH) 1.6], 3.89 [d, 9 H, POMe, *J*(PH) 10.4], 2.70 [d, 3 H, Mo=CMe, *J*(PH) 7.0], 2.65 [br, q, 1 H, C*H*Me, *J*(HH) 5.7], 2.35 (s, 3 H, CMe), 2.33 (s, 3 H, CMe), 2.17 [d, 3 H, CH*Me*, *J*(HH) 5.8 Hz]; ^{13}C-{^1H}, δ 305.5 [d, Mo=*C*Me, *J*(PC) 23.5], 132.5 (*C*Me), 108.5 (*C*Me), 101.3 (C_5H_5), 73.4 (*C*HMe), 57.2 [d, POMe, *J*(PC) 10.5], 29.5 [d, Mo=C*Me*, *J*(PC) 2.7], 18.0, 16.0, 15.1 (C*Me*), 15.1 [d, CH*Me*, *J*(PC) 1.9 Hz]; ^{31}P-{^1H}(CD_2Cl_2), δ 119.0 (POMe).

[Mo{=C(Me)-η³-[C(Me)C(Me)CHMe]}Cl{P(OMe)₃}(η-C_5H_5)][BF_4] 24. A reaction between the aqua complex **9** (0.09 g, 0.22 mmol) and $P(OMe)_3$ (24 μl, 0.22 mmol) in CH_2Cl_2 (20 cm^3) gave on similar work-up orange *crystals* of **24** (0.07 g, 68%) (Found: C, 39.7; H, 5.6. $C_{16}H_{27}BClF_4MoOP$ requires C, 39.6; H, 5.6%). NMR (CD_2Cl_2): ^1H, δ 5.76 [d, 5 H, C_5H_5, *J*(PH) 1.6], 3.81 [d, 9 H, POMe, *J*(PH) 10.4], 2.74 [d, 3 H, Mo=CMe, *J*(PH) 7.1], 2.65 [dq, 1 H, C*H*Me, *J*(HH) 6.0, *J*(PH) 9.5], 2.30 [dd, 3 H, CMe, *J*(PH) 1.0, *J*(HH) 1.2], 2.10 [d, 3 H, CH*Me*, *J*(HH) 6.0 Hz], 2.06 (s, 3 H, CMe); ^{13}C-{^1H}, δ 305.2 [d, Mo=*C*Me, *J*(PC) 23.0], 132.7 (*C*Me), 108.7 (*C*Me), 100.7 (C_5H_5), 75.1 (*C*HMe), 56.4 [d, POMe, *J*(PC) 10.4], 29.2 [d, Mo=C*Me*, *J*(PC) 2.1], 17.3, 15.0 (C*Me*), 14.7 [d, CH*Me*, *J*(PC) 1.0 Hz]; ^{31}P-{^1H}, δ 122.7 (POMe).

[Mo{=C(Et)-η³-[C(Et)(CEt)CHEt]}Br{P(OMe)₃}(η-C_5H_5)]-[BF_4] 25. Trimethyl phosphite (33 μl, 0.30 mmol) was added to a stirred solution of complex **11** (0.15 g, 0.30 mmol) in CH_2Cl_2 (10 cm^3). After 20 min the reaction mixture was filtered through Celite, the volume of the solvent reduced and the product precipitated with Et_2O. Recrystallisation from CH_2Cl_2–Et_2O gave orange *crystals* of **25** (0.175 g, 93%) (Found: C, 38.8; H, 5.8. $C_{20}H_{35}BBrF_4MoO_3P$ requires C, 38.9; H, 5.7%). NMR (CD_2Cl_2): ^1H, δ 5.87 [d, 5 H, C_5H_5, *J*(PH) 1.46], 3.85 [d, 9 H, POMe, *J*(PH) 10.3], 3.31 (m, 1 H, C*H*Et), 2.89 (m, 2 H, CH_2), 2.65 (m, 4 H, $2CH_2$), 2.46 (m, 2 H, CH_2), 1.50 [t, 3 H, Me, *J*(HH) 7.5], 1.45 [t, 3 H, Me, *J*(HH) 7.7], 1.23 [t, 3 H, Me, *J*(HH) 7.3], 0.92 [t, 3 H, Me, *J*(HH) 7.5 Hz]; ^{13}C-{^1H}, δ 307.2 [d, Mo=*C*Et, *J*(PC) 23.7], 135.0 (*C*Et), 110.6 (*C*Et), 100.2 (C_5H_5), 78.9 (*C*HEt), 56.6 [d, POMe, *J*(PC) 9.5], 37.4, 24.7, 23.5, 23.1 (CH_2), 15.8, 15.6, 14.2, 11.0 [d, Me, *J*(PC) 4.8 Hz]; ^{31}P-{^1H}, δ 119.2 (POMe).

Formation of complex 25 by reaction of complex 14 with trimethyl phosphite. Trimethyl phosphite (24 μl, 0.22 mmol) was added to a stirred solution of complex **14** (0.06 g, 0.11 mmol) in CH_2Cl_2 (10 cm^3). After 2 h the volume of the solvent was reduced, Et_2O added and the resultant precipitate recrystallised from CH_2Cl_2–Et_2O to give orange *crystals* of **25** (0.06 g, 88%).

[Mo{=C(Et)-η³-[C(Et)C(Et)CHEt]}Br(PMe_3)(η-C_5H_5)]-[BF_4] 26a. Trimethylphosphine (200 μl, 0.20 mmol of a 1.0 mol dm^{-3} solution in thf) was added dropwise with stirring to a solution of complex **14** (0.10 g, 0.2 mmol) in CH_2Cl_2 (10 cm^3). After 2 h at room temperature the volume of the solvent was reduced *in vacuo* and Et_2O added. The precipitate was recrystallised from CH_2Cl_2–Et_2O to give pink *crystals* of **26a** (0.10 g, 86%) (Found: C, 41.8; H, 6.3. $C_{20}H_{35}BBrF_4MoP$ requires C, 42.2; H, 6.2%). NMR (CD_2Cl_2): ^1H, δ 5.82 [d, 5 H, C_5H_5, *J*(PH) 1.6], 3.83–2.03 (m, 9 H, $4CH_2$, C*H*Et), 1.52 [d, 9 H, PMe, *J*(PH) 10.2], 1.50 [t, 3 H, Me, *J*(HH) 7.3], 1.42 [t, 3 H, Me, *J*(HH) 7.6], 1.22 [t, 3 H, Me, *J*(HH) 7.5], 0.87 [t, 3 H, Me, *J*(HH) 7.5 Hz]; ^{13}C-{^1H}, δ 299.1 [d, Mo=*C*Et, *J*(PC) 17.4] 133.7 (*C*Et), 111.7 (*C*Et), 100.0 (C_5H_5), 77.5 (*C*HEt), 37.5, 24.7, 24.1, 24.0 (CH_2), 17.5 [d, PMe, *J*(PC) 31.7], 16.1, 16.0, 14.5 (Me), 11.4 [d, Me, *J*(PC) 3.2 Hz]; ^{31}P-{^1H}, δ −5.25 (PMe). Mass spectra, *m/z*: FAB(+), $[M]^+$ 483.1, $[M - PMe_3]^+$ 407.0; FAB(−), BF_4^- 87.0.

Reaction of complex 11 with trimethylphosphine. Addition of PMe_3 (300 μl, 0.30 mmol of a 1.0 mol dm^{-3} solution in thf) to a stirred solution of the aqua complex **11** (0.15 g, 0.30 mmol) in CH_2Cl_2 (10 cm^3) gave a mixture (6:1) of the pink isomeric complexes **26a** and **26b** (0.13 g, 76%) (Found: C, 41.8; H, 6.3. $C_{20}H_{35}BBrF_4MoP$ requires C, 42.2; H, 6.2%). NMR (minor isomer **26b**, CD_2Cl_2): ^{13}C-{^1H}, δ 297.8 [d, Mo=*C*Et, *J*(PC) 16.3], 135.4 (*C*Et), 117.8 (*C*Et), 100.6 (C_5H_5), 82.1 (*C*HEt), 36.0 (CH_2), 23.2, 23.1, 21.6 (CH_2), 15.8, 15.7, 13.5 (Me), 14.9 [d, PMe, *J*(PC) 28.5], 12.5 [d, Me, *J*(PC) 3.9 Hz]; ^{31}P-{^1H}, δ −3.40 (PMe).

Reaction of complex 9 with trimethylphosphine. In a similar way addition of PMe_3 (200 μl, 0.20 mmol of a 1.0 mol dm^{-3} solution in thf) to a stirred solution of the aqua complex **9** (0.08 g, 0.20 mmol) in CH_2Cl_2 (10 cm^3) gave a mixture (6:1) of the orange isomeric complexes **27a** and **27b** (0.09 g, 80%) (Found: C, 40.4; H, 5.7. $C_{16}H_{27}BClF_4MoP$ requires C, 40.9; H, 5.8%). NMR (major isomer **27a**, CD_2Cl_2): ^1H, δ 5.74 [d, 5 H, C_5H_5, *J*(PH) 1.4], 2.70 [d, 3 H, Mo=C*Me*, *J*(PH) 5.2], 2.41 (m, 1 H, C*H*Me), 2.34 (s, 3 H, CMe), 2.12 [d, 2 H, CH*Me*, *J*(MeH) 6.0], 2.02 (s, 3 H, CMe), 1.44 [d, 9 H, PMe, *J*(PH) 10.4 Hz]; ^{13}C-{^1H}(CD_3NO_2), δ 297.9 [d, Mo=*C*Me, *J*(PC) 16.0], 130.9 (*C*Me), 111.3 (*C*Me), 101.7 (C_5H_5), 73.7 (*C*HMe), 29.1 (Mo=C*Me*), 17.5 (C*Me*), 17.0 (C*Me*), 16.4 [d, PMe, *J*(PC) 31.8 Hz], 15.2 (CH*Me*); ^{31}P-{^1H}, δ 0.27 (PMe). NMR (minor isomer **27b**, CD_2Cl_2): ^1H, δ 2.59 [d, 3 H, Mo=C*Me*, *J*(PH) 7.0],

Table 15 Crystallographic data for compounds **3**, **11**, **14**, **18**, **23**, **26a** and **28**

Complex	**3**	**11**	**14**	**18**	**23**	**26a**	**28**
Empirical formula	$C_{13}H_{17}IMo$	$C_{17}H_{28}BBrF_4OMo$	$C_{19}H_{29}BBrF_4NMo$	$C_{17}H_{26}Br_2Mo$	$C_{16}H_{27}O_3BBrF_4MoP$	$C_{20}H_{35}BBrF_4MoP$	$C_{16}H_{26}ClMoO_3P$
M	396.11	511.05	534.1	486.1	561.0	569.1	428.7
Crystal dimensions/mm	0.5 × 0.4 × 0.3	0.4 × 0.3 × 0.3	0.3 × 0.3 × 0.15	0.3 × 0.25 × 0.25	0.25 × 0.2 × 0.2	0.2 × 0.2 × 0.3	0.2 × 0.2 × 0.15
T/K	293(2)	170(2)	293(2)	293(2)	293(2)	293(2)	170(2)
λ/Å	0.710 73	0.709 30	0.709 30	0.710 69	0.710 69	0.709 30	0.709 30
Crystal system	Monoclinic	Triclinic	Monoclinic	Triclinic	Monoclinic	Monoclinic	Monoclinic
Space group	$P2_1/n$ (no. 14)	$P\bar{1}$ (no. 2)	$P2_1/n$ (no. 14)	$P\bar{1}$ (no. 2)	$P2_1/c$ (no. 14)	$P2_1/a$ (no. 14)	$P2_1/c$ (no. 14)
a/Å	8.4912(6)	10.107(2)	8.2124(6)	7.663(2)	12.429(7)	13.375(3)	14.311(5)
b/Å	13.648(2)	12.701(2)	9.259(1)	8.897(2)	11.408(3)	12.903(2)	8.801(3)
c/Å	12.245(2)	15.740(3)	28.930(3)	13.742(3)	15.719(7)	14.399(3)	14.873(4)
α/°	—	99.01(2)	—	89.34(3)	—	—	—
β/°	103.04(1)	99.21(1)	96.89(1)	98.82(2)	109.87(4)	94.28(1)	102.65(3)
γ/°	—	90.01(2)	—	93.72(2)	—	—	—
U/Å^3	1382.5	1969.2	2183.9	923.9	2096.1	2478.0	1827.8
Z	4	4	4	2	4	4	4
D_c/g cm^{-3}	1.903	1.724	1.62	1.75	1.78	1.53	1.56
μ(Mo-Kα)/mm^{-1}	3.151	2.734	2.47	5.02	2.66	1.24	0.96
F(000)	760	1024	1072	480	1120	1152	880
2θ range/°	4–50	4–48	4–48	4–44	4–48	4–48	4–48
Reflections collected	3243	6949	3948	2369	3576	4272	3195
No. unique data and n in $I \geqslant n\sigma(I)$	2442, 2	6173, 2	2407, 2	1413, 3	1859, 3	2229, 3	2091, 2
Absorption correction	ψ scans	DIFABS[28]	DIFABS[28]	DIFABS[28]	—	—	—
Max., min. absorption corrections	0.4810, 0.2734	1.114, 0.802	1.496, 0.907	1.302, 0.747	—	—	—
Refinement method	Full-matrix least squares	Block-matrix least-squares on F	Full-matrix least squares	Full-matrix least squares	Full-mattrix least squares	Full-matrix least squares	Full-matrix least squares
R	0.0398*	0.0698*	0.0429	0.0765	0.0819	0.0385	0.0495
R'	0.0955*	0.1599*	0.0417	0.0765	0.0819	0.0419	0.0512
Max., min. residual electron density/e Å^{-3}	0.70, −1.22	4.597, −2.780	0.37, −0.26	0.98, −1.00	0.86, −0.73	0.33, −0.18	0.51, −0.33
Weighting scheme	$w = 1/[\sigma^2(F_o^2) + (0.0453P)^2 + 1.2075P]$ where $P = (F_o^2 + 2F_c^2)/3$	$w = 1/[\sigma^2(F_o^2) + (0.0685P)^2 + 27.6991P]$ where $P = (F_o^2 + 2F_c^2)/3$	$w = 2.9464[\sigma^2(F) + 0.000\,352(F)^2]^{-1}$	Unit weights	Unit weights	$w = 1.5618[\sigma^2(F) + 0.001\,197(F)^2]^{-1}$	$w = 2.3416[\sigma^2(F) + 0.000\,941(F)^2]^{-1}$

Details in common: $R = \Sigma\,|\Delta|/\Sigma\,|F_o|$; $R' = (\Sigma\, w\Delta^2/\Sigma\, wF_o^2)^{\frac{1}{2}}$; $\Delta = F_o - F_c$. * $R1$ and $wR2$ quoted instead of R and R'.

2.41 (s, 3 H, C*Me*), 1.97 [d, 9 H, PMe, *J*(PH) 10.6 Hz] (η-C_5H_5 and C*H*Me signals obscured); ^{13}C-{^1H}(CD_3NO_2), δ 294.8 [d, Mo=*C*Me, *J*(PC) 20.0], 127.1 [d, *C*Me, *J*(PC) 5.4], 115.7 (*C*Me), 92.7 (C_5H_5), 54.5 (*C*HMe), 28.1 (Mo=C*Me*), 18.1 (C*Me*), 17.4 [d, PMe, *J*(PC) 32.0 Hz], 16.2 (CH*Me*); ^{31}P-{^1H}, δ 4.6 (PMe).

Reaction of complex 24 with Li[N(SiMe$_3$)$_2$]. Complex **24** (0.215 g, 0.42 mmol) was suspended in thf (15 cm^3), cooled to −78 °C and Li[N(SiMe$_3$)$_2$] (420 μl, 0.42 mmol of a 1.0 mol dm^{-3} solution in thf) was added dropwise with stirring, causing a change from orange to purple. The reaction mixture was allowed to warm to room temperature and after 2 h the volatiles were removed *in vacuo*. Extraction of the residue with pentane (3 × 10 cm^3), filtration through Celite and removal of the solvent gave a purple oil, which upon crystallisation (−30 °C) from pentane gave purple *crystals* of complex **28** (0.095 g, 52%) (Found: C, 44.4; H, 6.2. $C_{16}H_{26}ClMoO_3P$ requires C, 44.8; H, 6.1%). NMR(C_6D_6): ^1H, δ 5.39 [dd, 1 H, =C(*H*)H, *J*(PH) 3.3, *J*(HH) 0.9], 4.55 [d, 5 H, C_5H_5, *J*(PH) 1.4], 3.69 [dd, 1 H, =CH(*H*), *J*(PH) 2.0, *J*(HH) 0.9], 3.33 [d, 9 H, POMe, *J*(PH) 10.4], 2.39 [dd, 3 H, CH(*Me*)=C, *J*(PH) 2.0, *J*(HH) 0.9], 2.07 [dqq, 1 H, C*H*(Me)=C(Me), *J*(HH) 6.2, *J*(PH) 2.5, *J*(HH) 1.0], 1.91 (s, 3 H, CMe), 1.86 [d, 3 H, CH(*Me*)=C(Me), *J*(HH) 6.1 Hz]; ^{13}C-{^1H}, δ 196.5 [d, =*C*=CH$_2$, *J*(PC) 10.5], 129.1 (*C*Me), 103.6 (*C*Me), 93.0 (C_5H_5), 91.7 (C=*C*H$_2$), 65.2 (*C*HMe), 52.6 [d, POMe, *J*(PC) 6.1 Hz], 17.8 (C*Me*), 15.9 (C*Me*), 14.3 (C*Me*); ^{31}P-{^1H}, δ 169.9 (POMe). Mass spectrum, *m/z*: FAB(+), $[M]^+$ 429, $[M - Cl]^+$ 394, $[M - P(OMe)_3]^+$ 305.

Reaction of complex 28 with HBF$_4$·Et$_2$O. Dropwise addition (−78 °C) of HBF$_4$·Et$_2$O (77 μl, 0.52 mmol) to a stirred solution of complex **28** (0.23 g, 0.52 mmol) in CH_2Cl_2 (10 cm^3) resulted on warm up in a rapid change from purple to orange. Addition of Et_2O (10 cm^3) precipitated an orange solid, which on recrystallisation from CH_2Cl_2–Et_2O gave orange *crystals* of **24** (0.22 g, 95%) identified by comparison of the NMR spectra with that of an authentic sample.

[MoBr{η^4-CH(Me)=C(Me)C(Me)=CH(Me)}{P(OMe)$_3$}(η-C$_5$H$_5$)] 29. A solution of AlHBu$^i_2$ (0.36 mmol, mol dm^{-3} in hexane) was added (−78 °C) dropwise with stirring to a solution of complex **23** (0.20 g, 0.36 mmol) in thf (10 cm^3). On warming to room temperature the reaction mixture changed from orange to purple. The volatiles were removed *in vacuo*, the residue extracted into hexane (3 × 10 cm^3), filtered through Celite and then the hexane removed *in vacuo*. The residue was recrystallised (−30 °C) from hexane to give purple, air-sensitive *crystals* of **29** (0.13 g, 76%) (Found: C, 38.5; H, 5.9. $C_{16}H_{28}BrMoO_3P$ requires C, 38.3; H, 5.6%). NMR (C_6D_6): ^1H, δ 4.54 [d, 5 H, C_5H_5, *J*(PH) 1.3], 3.37 [d, 9 H, POMe, *J*(PH) 9.6], 2.35 [d, 3 H, C*Me*, *J*(PH) 2.0], 2.24 (s, 3 H, C*Me*), 1.89 [d, 3 H, CH*Me*, *J*(HH) 6.1], 1.29 [d, 3 H, CH*Me*, *J*(HH) 6.1], 1.25 [apparent q, 1 H, C*H*Me, *J*(HH) = *J*(PH) 6.2], 0.43 [apparent q, 1 H, C*H*Me, *J*(HH) = *J*(PH) 6.3 Hz]; ^{13}C-{^1H}, δ 116.3 (*C*Me), 112.0 (*C*Me), 89.9 (C_5H_5), 60.6 (*C*HMe), 57.6 (*C*HMe), 53.6 [d, POMe, *J*(PC) 9.0 Hz], 17.0 (C*Me*), 16.8 (CH*Me*), 16.1 (C*Me*), 15.4 (CH*Me*); ^{31}P-{^1H}, δ 143.8 (POMe). Mass spectrum, *m/z*: FAB(+), $[M]^+$ 473.0, $[M - P(OMe)_3]^+$ 352.0.

Reaction of complex 29 with [Ph$_3$C][BF$_4$]. A solution of [Ph$_3$C][BF$_4$] (0.036 g, 0.11 mmol) in CH_2Cl_2 (5 cm^3) was added (−78 °C) to a stirred solution of complex **29** (0.05 g, 0.11 mmol) in CH_2Cl_2 (10 cm^3). After warming to room temperature and stirring for 15 min the reaction mixture was filtered through Celite and the volume of the solvent reduced (3 cm^3) *in vacuo*. Addition of Et_2O precipitated an orange solid, which on recrystallisation (0 °C) from CH_2Cl_2–Et_2O gave orange *crystals* of **23** (0.04 g, 68%) identified by comparison of the NMR spectra with those of an authentic sample.

Crystal-structure determination

Many of the details of the crystal structure analyses carried out on compounds **3**, **11**, **14**, **18**, **23**, **26a** and **28** are collected in Table 15.

Data collection was performed on a CAD4 automatic four-circle diffractometer for complexes **11**, **14**, **26** and **28**. In the instance of compounds **18** and **23** data collections were carried out on a Hilger and Watts Y290 instrument, while data pertaining to complex **3** was obtained on a Siemans P4 diffractometer. All structures were solved using Patterson functions in SHELXS 86.[29] Refinements were executed using SHELX 76[30] except in the cases of **3** and **12**, which were refined using SHELXL 93.[31] Structural refinements were based on *F* with the exception of **3** where F^2 data were employed. Molecular plots were produced using ORTEX.[32] Hydrogen atoms were included at calculated positions where relevant except in the following cases: H(81) in **14**, was located in an advanced Fourier-difference electron-density map and refined at a distance of 0.96 Å from C(8), the hydrogen atom bonded to C(6) [H(61)] in **26** was similarly located and refined, H(61), H(101) and H(102) [attached to C(6) and C(10) respectively] in **28** were also located and positionally fixed in the final least-squares cycles. In complex **11** (where the asymmetric unit was seen to consist of two molecules), the hydrogens attached to C(9), C(9A) along with the protons in the water molecules precluded location as did the proton attached to C(9) in complex **23**.

All non-hydrogen atoms were treated anisotropically in the final least-squares cycles except for carbons 6, 7, 16 and 17 in compound **18**, where such refinement was not satisfactory.

As mentioned earlier, analysis of the supramolecular structure in **11** revealed that there was considerable interaction between the fluoroborate anions and the ligated water molecules contained in the cations. In particular, O(1) in the asymmetric unit as presented was seen to interact with fluorines F(1) and F(7) of the anions generated *via* the operators. $-1 - x, y, z$ and $1 - x, 1 - y, 2 - z$ respectively [O(1)···F(1) 2.68(1), O(1)···F(7), 2.74(1) Å]. Similarly, O(2) was observed to interact with F(3) of the same asymmetric unit, and with F(6) of the anion generated *via* the $2 - x, 1 - y, 2 - z$ transformation [O(2)···F(3) 2.78(1), O(2)···F(6) 2.81(13) Å]. Although, as previously mentioned, the water protons could not be reliably located in this molecule, it is reasonable to suggest that the above contacts are in fact indicative of hydrogen bonding. A packing diagram for this complex is given in Fig. 3.

Atomic coordinates, thermal parameters, and bond lengths and angles have been deposited at the Cambridge Crystallographic Data Centre (CCDC). See Instructions for Authors, *J. Chem. Soc., Dalton Trans.*, 1996, Issue 1. Any request to the CCDC for this material should quote the full literature citation and the reference number 186/282.

Extended-Hückel molecular orbital calculations

The calculations were performed using the extended-Hückel iterative method on the CAChe system using the standard STO-3G basis set and a Wolfenburg–Helmhotz constant, *k*, of 1.75. The EHT parameters in the CAChe library are based upon experimental data.[33]

Acknowledgements

We thank the SERC (EPSRC) for support and for studentships (to C. B. M. N., A. P. W. and C. M. W.). We also thank Rhodri Ll. Thomas for his support and Professor A. J. Welch for use of the facilities at the Heriot-Watt University.

References

1 Part 63. G. Brauers, F. J. Feher, M. Green, J. K. Hogg and A. G. Orpen, *J. Chem. Soc., Dalton Trans.*, 1996, 3387.

2 M. Crocker, M. Green, A. G. Orpen, H.-P. Neumann and C. J. Schaverien, *J. Chem. Soc., Chem. Commun.*, 1984, 1351.
3 M. Crocker, M. Green, K. R. Nagle, A. G. Orpen, H.-P. Neumann, C. E. Morton and C. J. Schaverien, *Organometallics*, 1990, **9**, 1422.
4 J. R. Morrow, T. L. Tonker and J. L. Templeton, *J. Am. Chem. Soc.*, 1985, **107**, 5004.
5 L. Carlton, J. L. Davidson, P. Ewing, L. Manojlovic-Muir and K. W. Muir, *J. Chem. Soc., Chem. Commun.*, 1985, 1474; N. M. Agh-Atabay, J. L. Davidson and K. W. Muir, *J. Chem. Soc., Chem. Commun.*, 1990, 1399; L. Carlton, N. M. Agh-Atabay and J. L. Davidson, *J. Organomet. Chem.*, 1991, **413**, 205; N. M. Agh-Atabay and J. L. Davidson, *J. Chem. Soc., Dalton Trans.*, 1992, 3531.
6 G. C. Conole, M. Green, M. McPartlin, C. Reeve and C. M. Woolhouse, *J. Chem. Soc., Chem. Commun.*, 1988, 1310.
7 W. Y. Yeh, S. M. Ping and L.-K. Liu, *Inorg. Chem.*, 1993, **32**, 2965.
8 F. Biasotto, M. Etienne and F. Dahan, *Organometallics*, 1995, **14**, 1870.
9 C. Carfagna, N. Carr, R. J. Deeth, S. J. Dossett, M. Green, M. F. Mahon and C. Vaughan, *J. Chem. Soc., Dalton Trans.*, 1996, 415.
10 S. J. Dossett, M. Green, M. F. Mahon and J. M. McInnes, *J. Chem. Soc., Chem. Commun.*, 1995, 767.
11 R. J. Deeth, S. J. Dossett, M. Green, M. F. Mahon and S. J. Rumble, *J. Chem. Soc., Chem. Commun.*, 1995, 593.
12 J. L. Davidson, M. Green, F. G. A. Stone and A. J. Welch, *J. Chem. Soc., Dalton Trans.*, 1976, 738.
13 A. G. Orpen, L. Brammer, F. H. Allen, O. Kennard, D. G. Watson and R. Taylor, *J. Chem. Soc., Dalton Trans.*, 1989, S1.
14 S. R. Allen, R. G. Beevor, M. Green, N. C. Norman, A. G. Orpen and I. D. Williams, *J. Chem. Soc., Dalton Trans.*, 1985, 435.
15 S. R. Allen, R. G. Beevor, M. Green, A. G. Orpen, K. E. Paddick and I. D. Williams, *J. Chem. Soc., Dalton Trans.*, 1987, 591.
16 B. C. Ward and J. L. Templeton, *J. Am. Chem. Soc.*, 1980, **102**, 1432.
17 R. V. Honeychuck and W. H. Hersch, *Inorg. Chem.*, 1989, **28**, 2869.
18 K. H. Dötz, *Angew. Chem., Int. Ed. Engl.*, 1984, **23**, 587.
19 P. Hofmann and J. Hämmerle, *Angew. Chem., Int. Ed. Engl.*, 1989, **28**, 908.
20 W. Clegg, M. Green, C. A. Hall, D. C. R. Hockless, N. C. Norman and C. M. Woolhouse, *J. Chem. Soc., Chem. Commun.*, 1990, 1330.
21 S. A. Benyunes, R. J. Deeth, A. Fries, M. Green, M. McPartlin and C. B. M. Nation, *J. Chem. Soc., Dalton Trans.*, 1992, 3453.
22 M. Murakemi, K. Itami and Y. Ito, *Angew. Chem., Int. Ed. Engl.*, 1995, **34**, 2691.
23 L. S. Trifonov, A. S. Orahovats, R. Trewo and H. Heimgartner, *Helv. Chim. Acta*, 1988, **71**, 551.
24 S. P. Saberi and S. E. Thomas, *J. Chem. Soc., Perkin Trans. 1*, 1992, 259.
25 M. Green, M. F. Mahon, K. C. Molloy, C. B. M. Nation and C. M. Woolhouse, *J. Chem. Soc., Chem. Commun.*, 1991, 1587.
26 J. C. Hayes and N. J. Cooper, *J. Am. Chem. Soc.*, 1982, **104**, 5570.
27 S. R. Allen, P. K. Baker, S. G. Barnes, M. Green, L. Trollope, L. M. Manojlovic-Muir and K. W. Muir, *J. Chem. Soc., Dalton Trans.*, 1981, 873.
28 N. G. Walker and D. Stuart, DIFABS, *Acta Crystallogr., Sect. A*, 1983, **39**, 158.
29 G. M. Sheldrick, *Acta Crystallogr., Sect. A*, 1990, 467.
30 G. M. Sheldrick, SHELX 76, a computer program for crystal structure determination, University of Cambridge, 1976.
31 G. M. Sheldrick, SHELXS 93, University of Göttingen, 1993.
32 P. McArdle, *J. Appl. Crystallogr.*, 1994, **27**, 438.
33 CAChe system, a comprehensive package of molecular modelling and computational tools developed by CAChe Scientific Inc., Beaverton, OR.

Received 13*th June* 1996; *Paper* 6/04159K